Variability and stability of anthropogenic CO2 in Antarctic Bottom Waters observed in the Indian sector of the Southern

Léo Mahieu, Claire Lo Monaco, Nicolas Metzl, Jonathan Fin, Claude Mignon

https://doi.org/10.5194/os-2020-37
Preprint. Discussion started: 4 May 2020

Ocean Science
Discussions
Open Access
EGU

Variability and stability of anthropogenic CO2 in Antarctic Bottom Waters observed in the Indian sector of the Southern Ocean, 1978-2018

Léo Mahieu[1], Claire Lo Monaco[2], Nicolas Metzl[2], Jonathan Fin[2], Claude Mignon[2]

[1]Ocean Sciences, School of Environmental Sciences, 4 Brownlow Street, Liverpool L69 3GP, UK
[2]LOCEAN-IPSL, CNRS, Sorbonne Université, Paris, France

Correspondence to: Léo Mahieu (Leo.Mahieu@live.fr); Claire Lo Monaco (claire.lomonaco@locean.upmc.fr)

Abstract

Antarctic bottom waters (AABWs) are known as a long term sink for anthropogenic CO_2 (C_{ant}) but is hardly quantified because of the scarcity of the observations, specifically at an interannual scale. We present in this manuscript an original dataset combining 40 years of carbonate system observations in the Indian sector of the Southern Ocean (Enderby Basin) to evaluate and interpret the interannual variability of C_{ant} in the AABW. This investigation is based on regular observations collected at the same location (63° E/56.5° S) in the frame of the French observatory OISO from 1998 to 2018 extended by GEOSECS and INDIGO observations (1978, 1985 and 1987).

At this location the main sources of AABW sampled is the fresh and younger Cape Darnley bottom water (CDBW) and the Weddell Sea deep water (WSDW). Our calculations reveal that C_{ant} concentrations increased significantly in AABW, from about +7 µmol.kg^{-1} in 1978-1987 to +13 µmol.kg^{-1} in 2010-2018. This is comparable to previous estimates in other SO basins, with the exception of bottom waters close to their formation sites where C_{ant} concentrations are about twice as large. Our analysis shows that the C_T and C_{ant} increasing rates in AABW are about the same over the period 1978-2018, and we conclude that the long-term change in C_T is mainly due to the uptake of anthropogenic CO_2 in the different formation regions. This is however modulated by significant interannual to pluriannual variability associated with variations in hydrological (Θ, S) and biogeochemical (C_T, A_T, O_2) properties. A surprising result is the apparent stability of C_{ant} concentrations in recent years despite the increase in C_T and the gradual acceleration of atmospheric CO_2.

The C_{ant} sequestration by AABWs is more variable than expected and depends on a complex combination of physical, chemical and biological processes at the formation sites and during the transit of the different AABWs. The interannual variability at play in AABW needs to be carefully considered on the extrapolated estimation of C_{ant} sequestration based on sparse observations over several years.

1 Introduction

CO_2 atmospheric concentration has been increasing since the start of the industrialization (Keeling and Whorf, 2000). This increase leads to an ocean uptake of about a quarter of C_{ant} emissions (Le Quéré et al., 2018; Gruber et al., 2019a). It is widely acknowledged that the Southern Ocean (SO) is responsible for 40 % of the C_{ant} ocean sequestration (Gruber et al., 2009; Khatiwala et al., 2009; Matear, 2001; McNeil et al., 2003; Orr et al., 2001). Ocean C_{ant} uptake and sequestration have the benefit to limit the atmospheric CO_2 increase but also result in a

https://doi.org/10.5194/os-2020-37
Preprint. Discussion started: 4 May 2020

gradual decrease of the ocean pH (Gattuso and Hansson, 2011; Jiang et al., 2019). Understanding the oceanic C_{ant} sequestration and its variability is of major importance to predict future atmospheric CO_2 concentrations, impact on the climate and impact of the pH change on marine ecosystems (de Baar, 1992; Orr et al., 2005; Ridgwell and Zeebe, 2005).

C_{ant} in seawater cannot be measured directly and the evaluation of the relatively small C_{ant} signal from the total inorganic dissolved carbon (C_T; around 3 %; Pardo et al, 2014) is still a challenge to overcome. Different approaches have been developed in the last 40 years to quantify C_{ant} concentrations in the oceans. The 'historical' back calculation method based on C_T measurement and preformed inorganic carbon estimate (C^0) was independently published by Brewer (1978) and Chen and Millero (1979). This method has been often applied at regional and basin scale (Chen, 1982, 1993; Goyet et al., 1998; Körtzinger et al., 1998, 1999; Poisson and Chen, 1987; Lo Monaco et al., 2005a). More recently the TrOCA method (Tracer combining Oxygen, dissolved Carbon and total Alkalinity) has been developed (Touratier and Goyet, 2004a, 2004b; Touratier et al., 2007) and applied in various regions including the SO (e.g. Lo Monaco et al., 2005b; Sandrini et al., 2007; Pardo et al., 2014; Roden et al., 2016; Shadwick et al., 2014; Van Heuven et al., 2011; Kerr et al., 2018). Comparisons with other data-based methods show significant differences in C_{ant} concentrations, especially at high latitudes and more particularly in deep and bottom waters (Lo Monaco et al., 2005b; Vázquez-Rodríguez et al., 2009; Pardo et al., 2014). Thus, there is a need to better explore the C_T and C_{ant} temporal variability in the deep ocean, especially in the SO where observations are relatively sparse.

Antarctic bottom waters (AABWs) are of specific interest for the atmospheric CO_2 and heat regulation as they play a major role in the meridional overturning circulation (Johnson et al., 2008; Marshall and Speer, 2012) . AABWs represent a large volume of water by covering the majority of the bottom world ocean (Mantyla and Reid, 1995), and their spreading in the interior ocean through circulation and water mixing (Siegenthaler and Sarmiento, 1993) is a key mechanism for the long-term sequestration of C_{ant} and climate regulation. The AABW formation is a specific process occurring in few locations around the Antarctic continent (Orsi et al., 1999). In short, the AABW formation occurs when the Dense Shelf Water (DSW) flows down along the continental shelf. The DSW density required for this process to happen is reached by the increase in salinity (S) due to brine release from the ice formation and by a decrease in temperature due to heat loss to either the ice-shelf or the atmosphere. Importantly, AABW formation process is enhanced by katabatic winds that open areas free of ice called polynyas (Williams et al., 2007). Indeed, katabatic winds are responsible for an intense cooling that enhance the formation of ice constantly pushed away by the wind, leading to cold and salty surface waters in contact with the atmosphere. The variable conditions of wind, ice production, surface water cooling and continental slope shape encountered around the Antarctic continent lead to different types of AABW, hence the AABW characteristics can be used to identify their formation sites.

The ability of AABW to accumulate C_{ant} has been controversial since one can believe that the ice coverage limits the invasion of C_{ant} in Antarctic surface waters (e.g. Poisson and Chen, 1987). This is however not the case in polynyas, and several studies have reported significant C_{ant} signals in AABW formation regions, likely due to the uptake of CO_2 induced by high primary production (Roden et al., 2016; Sandrini et al., 2007; Shadwick et al., 2014; van Heuven et al., 2011, 2014). However, little is known about the variability and evolution of CO_2 fluxes in AABW formation regions, and since biological and physical processes are strongly impacted by seasonal and interannual climatic variations (Fukamachi et al., 2000; Gordon et al., 2010, 2015; Gruber et al., 2019b; McKee et

https://doi.org/10.5194/os-2020-37
Preprint. Discussion started: 4 May 2020

al., 2011), the amount of C_{ant} stored in the AABWs may be very variable, which could bias the estimates of C_{ant} trends derived from data sets collected several years apart (e.g. Williams et al., 2015; Pardo et al., 2017; Murata et al., 2019).

In this context of potentially high variability in C_{ant} uptake at AABW formation sites, as well as in AABW export, circulation and mixing, we used repeated observations collected in the Indian sector of the Southern Ocean to explore the variability in C_{ant} and C_T in AABW and evaluate their evolution over the last 40 years.

2 Studied area

2.1 AABW samples during the last 40 years

Most of the data used in this study were obtained in the frame of the long-term observational project OISO (Ocean Indien Service d'Observations) conducted since 1998 onboard the R.S.V. Marion-Dufresne (IPEV/TAAF). During these cruises, several stations are visited, but only one station is sampled down to the bottom (4800 m) south of the Polar Front at 63.0° E and 56.5° S (hereafter noted OISO-ST11). This station is located in the Enderby Basin on the Western side of the Kerguelen Plateau (Fig. 1) and coincides with the station 75 of the INDIGO-III cruise (1987). In our analysis, we also included data from the station 14 of the INDIGO-I cruise (1985) and the station 430 of the GEOSECS cruise (1978) located near OISO-ST11 site (405 km and 465 km respectively). All the re-occupations used in this analysis are listed in Table 1.

Table 1.

2.2 AABWs circulation in the Atlantic and Indian sectors of the Southern Ocean

The circulation in the SO is mainly governed by the ACC that flows Eastward, while the Coastal Antarctic Current (CAC) flows Westward (Fig. 1). The ACC and the CAC influence the circulation of the entire water column, including the AABWs. The main AABW formation sites are the Weddell Sea where are produced deep and bottom waters (WSDW and WSBW, respectively; Gordon, 2001; Gordon et al., 2010), the Ross Sea (RSBW; Gordon et al., 2015, 2009), the Adelie Land coast (ALBW; Williams et al., 2008, 2010) and the Cape Darnley Polynya (CDBW; Ohshima et al., 2013). AABW formation in the Prydz Bay has also been observed (Rodehacke et al., 2007; Yabuki et al., 2006) from three polynyas and two ice shelves flowing into the Prydz Channel (Williams et al., 2016) and mixing with the CDBW. The CDBW and Prydz Bay bottom waters (hereafter called CDBW) represent a significant AABW export (13 % of all AABWs exports; Ohshima et al., 2013).

The largest bottom water source of the global ocean is the Weddell Sea (Gordon et al., 2001). The exported WSDW is a mixture of the Warm Deep Water (WDW) and the WSBW. The WSDW in the ACC and Weddell Gyre mixes with the Circumpolar Deep Water (CDW). A part of the WSDW deflecting southward with the ACC in the Enderby Basin reaches the Princess Elizabeth Trough (PET) region, East of the Kerguelen Plateau, where it mixes with other types of AABWs (Orsi et al., 1999).

In the PET sector, the CAC transports a mixture of RSBW and ALBW and accelerates Northward along the Eastern side of the Kerguelen Plateau (Mantyla and Reid, 1995; Fukamachi et al., 2010). Part of the ALBW-RSBW mixture also reaches the Western side of the Kerguelen Plateau (Orsi et al., 1999; Van Wijk and Rintoul, 2014) and mix with the CDBW. The mixture of CDBW and ALBW-RSBW either flows Westward with the CAC and dilutes with

https://doi.org/10.5194/os-2020-37
Preprint. Discussion started: 4 May 2020

the CDW (Meijers et al., 2010) or flow Northward (Ohshima et al., 2013) and mix with the older WSDW before reaching the location of our time-series station in the eastern Enderby Basin.
Figure 1.

2.3 AABW definition

Nowadays, the distinction of water masses is usually performed according to neutral density (γ^n) layers. In the SO, CDW and AABW properties are generally well defined in the range 28.15-28.27 kg.m^{-3} and 28.27-bottom respectively (Orsi et al., 1999; Murata et al 2019). However, to interpret the long-term variability of the properties in the AABWs at our location, we prefer to adjust the AABW layer in a narrow band, and select the samples for γ^n > 28.35 kg.m^{-3} (range starting at 4200m to 4600m depending on the year, see Fig. 3). γ^n > 28.35 kg.m^{-3} corresponds to the AABW characteristics observed at higher latitudes in the Indian SO sector (Roden et al., 2016).

2.4 AABW composition at OISO-ST11

At each formation site, AABWs experienced significant temporal property changes, mostly recognized at decadal scale (e.g. freshening in the South Indian Ocean, Menezes et al., 2017) with potential impact on carbon uptake and C_{ant} concentrations during AABW formation (Shadwick et al., 2013). The Θ-S diagram constructed from yearly averaged data in bottom waters (Fig. 2) shows that the AABW at OISO-ST11 is a complex mixture of WSDW, CDBW, RSBW and ALBW. The coldest type of AABW was observed at the GEOSECS station at 60° S (-0.56 °C), probably because it experienced less mixing with CDW compared to the warmer type of AABW observed at the INDIGO-1 station at 53° S (-0.44 °C). For the other cruises and years, Θ in AABW ranges from -0.51 to -0.45 °C with no clear indication on the specific AABW origin. The S range observed in the bottom waters at OISO-ST11 (34.65-34.67), illustrates either changes in mixing with various AABW sources or temporal variations at the formation site. Given the knowledge of deep and bottom waters circulation and characteristics (Fig.s 1 and 2) and the significant C_{ant} concentrations that we estimated at depth (Fig. 3), the main contribution at our location is likely the younger and colder CDBW for which relatively high C_{ant} concentrations have been recently documented (Roden et al., 2016). From its formation region, the CDBW can either flow westward with the CAC or flow northward in the Enderby Basin (Ohshima et al., 2013, Fig. 1). In the CAC branch, the CDBW mixes with the CDW along the Antarctic shelf and the continental slope between 80°E and 30°E (Meijers et al., 2010; Roden et al., 2016). On the western side of the Kerguelen Plateau, CDBW also mixes with RSBW and ALBW (Orsi et al., 1999; Van Wijk and Rintoul, 2014). In this context, the C_{ant} concentrations observed in the bottom layer at OISO-ST11 are probably not linked to a single AABW source, but are likely a complex interplay of AABW from different sources with different biogeochemical properties.
Figure 2.

3 Material and methods

3.1 Validation of the data

For 1998-2004, the OISO data were quality controlled in CARINA (Lo Monaco et al., 2010) and for 2005 and 2009-2011 in GLODAPv2 (Key et al., 2015; Olsen et al., 2016, 2019). The 3 additional stations from GEOSECS and INDIGO were qualified in GLODAP-v1 (Key et al., 2004) and previously used for the first C_{ant} estimates in

https://doi.org/10.5194/os-2020-37
Preprint. Discussion started: 4 May 2020

the Indian Ocean (Sabine et al., 1999). The data for INDIGO III (1987) have been revisited in GLODAP-v2 but the correction applied on A_T values leads to a suspicious offset and we decided to use the adjustment proposed in GLODAP-v1 and confirmed in CARINA.

For the recent OISO cruises conducted in 2012-2018 not yet qualified in the GLODAP project, we have proceeded to a data control mainly based on repeated observations in deep waters (CDW) where C_{ant} concentrations are low and subject to very small changes from year to year. At this location, the seasonal variations of all properties are only observed in the mixed-layer, about 50 m in austral summer and 150 m in winter (Metzl et al., 2006). Therefore, for deep water analysis, we used the observations available for all seasons (Table 1).

3.2 Biogeochemical measurements

Measurement methods during OISO cruises were previously described (Jabaud-Jan et al., 2004; Metzl et al., 2006). In short, measurements were obtained using Conductivity-Temperature-Depth (CTD) casts fixed on a 24 bottles rosette equipped with 12 L General Oceanics Niskin bottles. Θ (in °C) and S (no unit) measurements have an accuracy of 0.01 of their respective units. C_T and A_T were sampled in 500 mL glass bottles and poisoned with 100 µL of $HgCl_2$ saturated solution to halt biological activity. Discrete C_T and A_T samples were analyzed onboard by potentiometric titration derived from the method developed by Edmond (1970) using a closed cell. The accuracy for C_T and A_T varies from 1 to 3.5 µmol.kg^{-1} (depending on the cruise) and is determined by sample duplicates in surface, at 1000 m and bottom waters. All measurements were calibrated with Certified Reference Materials (CRMs) provided by A.G. Dickson laboratory (Scripps Institute of Oceanography). O_2 was determined by an oxygen sensor fixed on the rosette. These values were adjusted using measurements obtained by Winkler titrations using a potentiometric titration system (at least 12 measurements for each profile). Thiosulphate solution used in Winkler titration was calibrated using iodate standard solution to provide the standard O_2 accuracy of 2 µmol.kg^{-1}. Nitrate (NO_3) and Silicate (Si) were measured onboard or offshore with an automatic colorimetric Technicon analyser following the methods described by Tréguer and Le Corre (1975) until 2008, and the revised protocol described by Aminot and Kérouel (2007) since 2009. Based on replicate measurements for deep samples we estimate an error of about 0.3 % for both nutrients. NO_3 concentrations are not available for all the cruises used in this analysis. The mean NO_3 concentrations in the AABW at OISO-ST11 is 32.8 ± 1.2 µmol.kg^{-1} while the average value derived from GLODAP-v2 database in bottom waters south of 50°S in the South Indian is 32.4 ± 0.6 µmol.kg^{-1}. The lack of NO_3 for few cruises has been palliated by considering a standard value of 33 µmol.kg^{-1} with a limited impact on C_{ant} determined by the C° method (from 0.1 µmol.kg^{-1} to 1.7 µmol.kg^{-1} on the mean annual values).

3.3 C_{ant} calculation using the TrOCA method

The TrOCA method was first presented by Touratier and Goyet (2004a, 2004b) and revised by Touratier et al. (2007). Following the concept of the quasi-conservative tracer NO (Broecker, 1974), TrOCA is a tracer defined as a combination of O_2, C_T and A_T, following:

$$TrOCA = O_2 + a\left(C_T - \frac{1}{2}A_T\right), \quad (1)$$

where a is the Redfield ratio.

https://doi.org/10.5194/os-2020-37
Preprint. Discussion started: 4 May 2020

The temporal change in TrOCA is independent of biological processes and can be attributed to anthropogenic carbon (Touratier and Goyet, 2004a). Therefore, C_{ant} can be directly calculated from the difference between TrOCA and its pre-industrial value TrOCA°:

$$C_{ant} = \frac{TrOCA - TrOCA^0}{a}, \quad (2)$$

where TrOCA° is evaluated as a function of θ and A_T (Eq. 3):

$$TrOCA^0 = e^{\left[b-(c).\Theta-\frac{d}{{A_T}^2}\right]}, \quad (3)$$

In these expressions, coefficients a, b, c and d were adjusted by Touratier et al. (2007) from free anthropogenic CO_2 deep waters using the tracers $\Delta^{14}C$ and CFC-11 from the GLODAP-V1 database (Key et al., 2004). The final expression used to calculate C_{ant} is:

$$C_{ant} = \frac{O_2 + 1{,}279\left(C_T - \frac{1}{2}A_T\right) - e^{\left[7{,}511-(1{,}087.10^{-2}).\Theta-\frac{7{,}81.10^5}{{A_T}^2}\right]}}{1{,}279}, \quad (4)$$

The consideration of the errors on the different parameters involved in the TrOCA method results in an uncertainty of ±6.25 µmol.kg^{-1} (mostly due to the parameter a, leading to ±3.31 µmol.kg^{-1}). As this error is relatively large compared to the expected Cant concentrations in deep and bottom SO waters (Pardo et al., 2014) we will compare the TrOCA results using another indirect method to interpret Cant changes over 40 years.

3.4 C_{ant} calculation using the preformed inorganic carbon method

To support the C_{ant} trend determined with the TrOCA method, C_{ant} was also estimated using a back-calculation approach noted C° (Brewer, 1978; Chen and Millero, 1979), previously adapted for C_{ant} estimates along the WOCE-I6 section between Africa and Antarctica (Lo Monaco et al., 2005a). This method consists in the correction of the measured C_T for the biological contribution (C_{bio}) and the preindustrial preformed C_T ($C_{0,PI}$):

$$C_{ant} = C_T - C_{bio} - C_{0,PI}, \quad (5)$$

C_{bio} (Eq. 6) depends on carbonate dissolution and organic matter remineralization, taking account of the corrected Redfield ratio from Kortzinger et al. (2001):

$$C_{bio} = 0.5\Delta A_T - (C/O_2 + 0.5N/O_2)\Delta O_2, \quad (6)$$

Where C/O_2 = 106/138 and N/O_2 = 16/138. ΔA_T and ΔO_2 are the difference between the measured values (A_T and O_2) and the preindustrial values (A_T^0 and O_2^0). A_T^0 (Eq. 7) has been computed by Lo Monaco et al. (2005a) as a function of Θ, S and the conservative tracer PO:

$$A_T^0 = 0.0685PO + 59.79S - 1.45\Theta + 217.1, \quad (7)$$

PO (Eq. 8) has been defined by Broecker (1974) and depends on the equilibrium of O_2 with phosphate (PO_4). When PO_4 data are not available, nitrate (NO_3) can be used instead (Anderson and Sarmiento, 1994):

$$PO = O_2 + 170PO_4 = O_2 + 170/16NO_3, \quad (8)$$

To determine O_2^0, it is assumed that the surface water is in full equilibrium with the atmosphere (O_2^0=$O_{2,sat}$; Benson and Krause, 1980) and after only impacted by the biological activity (Weiss, 1970). The correction of $O_{2,sat}$ has been proposed by Lo Monaco et al. (2005a) to take account of the undersaturation of O_2 due to sea-ice cover. ΔO_2 is, therefore, corrected by assuming a mean mixing ratio of the ice-covered surface waters k=50 % (Lo Monaco et al., 2005a), and a mean value for O_2 undersaturation in ice-covered surface waters α=12 % (Anderson et al., 1991) according to Eq. 9:

https://doi.org/10.5194/os-2020-37
Preprint. Discussion started: 4 May 2020

$$\Delta O_2 = (1 - \alpha k) O_{2,sat} - O_2 = AOU \,, \quad (9)$$

$C_{0,PI}$ in equation 5 is a function of the current preformed C_T ($C_{0,obs}$) and a reference water term (Eq. 10):

$$C_{0,PI} = C_{0,obs} + \left[C_T - C_{bio} - C_{0,obs}\right]_{REF} \,, \quad (10)$$

Where the reference water term has been computed using an optimum multiparametric (OMP) model and defined as 51 µmol.kg^{-1} from North Atlantic deep water (Lo Monaco et al., 2005a) and $C_{0,obs}$ has been computed similarly as A_T^0 (Eq. 11):

$$C_{0,obs} = -0.0439PO + 42.79S - 12.02\Theta + 739.8 \,, \quad (11)$$

For more details in the C° method, which has a final error of ± 6 µmol.kg^{-1}, especially on the determination of reference water terms and on the errors of this method, please see Lo Monaco et al. (2005a).

4. Results

The vertical distribution of hydrological and biogeochemical properties observed in deep and bottom waters and their evolution over the last 40 years are displayed in Fig. 3. The LCDW layer (γ^n = 28.15-28.27 kg.m^{-3}) is characterized by maximum AOU values (Fig. 3c), maximum C_T concentrations (Fig. 3d) and minimum C_{ant} concentrations (Fig. 3a). C_{ant} concentrations were not significant in the LCDW until the end of the 1990s (<6 µmol.kg^{-1}), then our data show a sudden increase in C_{ant} between January and December 1998, followed by relatively constant C_{ant} concentrations (10±3 µmol.kg^{-1}). In the core of AABW (γ^n > 28.35 kg.m^{-3}), well identified by low Θ, low S, high O_2 and low AOU, C_{ant} concentrations are higher than in the overlying deep waters (Fig. 3a) and increased from 5±4 µmol.kg^{-1} in 1978, 7±4 µmol.kg^{-1} in the mid-1980s to 13±2 µmol.kg^{-1} at the end of the 1990s and up to 19±2 µmol.kg^{-1} in 2004 (Fig. 4a). Figure 4a also shows a very good agreement between the TrOCA method and the C^0 method for both the magnitude and variability of C_{ant} in the core of AABW. Our results show a mean C_{ant} trend in AABW of +1.6 µmol.kg^{-1}.decade^{-1} over the full period and a maximum trend of the order of +6.5 µmol.kg^{-1}.decade^{-1} over 1987-2004 (Table 2). These trends are lower than the theoretical trend expected from the increase in atmospheric CO_2. Indeed, assuming that the surface ocean fCO_2 follows the atmospheric growth rate (+1.8 µatm.year^{-1} over 1978-2018), the theoretical C_{ant} trend at the AABW formation sites would be of the order of +8 µmol.kg^{-1}.decade^{-1}. The observed slow C_{ant} trends can be partly explained by the transit time for AABW to reach our study site and the mixing of AABW with older CDW waters that contain less C_{ant} (Fig. 3).

Figure 3.

To investigate changes in the accumulation of C_{ant} in AABW, Fig. 4 shows the evolution of C_T, A_T, O_2, Θ and S (properties used to estimate C_{ant}), as well as the "natural" component of C_T (C_{Tnat} calculated as the difference between C_T and C_{ant}). Over the full period, C_T increased by 2.0±0.5 µmol.kg^{-1}.decade^{-1}, mostly due to the accumulation of C_{ant} (Table 2). Our data also show a significant decrease in O_2 concentrations by 0.8±0.4 µmol.kg^{-1}.decade^{-1} over the 40-years period (Fig. 4c) that could be caused by reduced ventilation, as suggested by Schmidtko et al. (2017) who observed significant O_2 loss in the global ocean. In the deep Indian SO sector, these authors found a trend approaching -1 µmol.kg^{-1}.decade^{-1} over 50 years (1960-2010), which is consistent with our data. We did not detect any significant trend in A_T, Θ and S over the full period, but on shorter periods our data show a significant decrease in A_T from the mid-1980s to 2004 (Fig. 4d, Table 2) that is also observed in the overlying deep waters (Fig. 3f). This could suggest reduced calcification in the upper ocean leading to less sinking of calcium carbonate tests and hence a decrease in C_{Tnat} (i.e. for this period the increase in C_T was lower than the

https://doi.org/10.5194/os-2020-37
Preprint. Discussion started: 4 May 2020

accumulation of C_{ant}). This event is followed by an increase in C_{Tnat} since 2004 associated to a rapid decrease in O_2 (increase in AOU) and a decrease in C_{ant} (Table 2). These recent trends were associated with a small increase in θ (Fig. 4e, Table 2), but no significant trend in S (Fig. 4f). The increase in C_{Tnat} is thus unlikely originating solely from increased mixing with LCDW during bottom waters transport. Enhanced organic matter remineralization is also unlikely since nitrate did not show any significant trend (Table 2).

Table 2.

Figure 4.

Importantly, our data show substantial interannual variations in AABW properties, which could significantly impact the trends estimated from limited reoccupations (e.g. Williams et al., 2015; Pardo et al., 2017; Murata et al., 2019). For example, we found relatively higher C_{ant} concentrations in 1985 (10 µmol.kg^{-1}) compared to 1978 and 1987 (5 µmol.kg^{-1}). This is linked to a signal of low S in 1985 that could be due to a larger contribution of fresher AABW or reduced mixing with saltier LCDW (Fig. 3h). Over the last decade (2009-2018), our data show large and rapid changes in S that are partly reflected on C_T and O_2, and that could explain the relatively low C_{ant} concentrations observed over this period. Indeed, the S maximum observed in 2012 (correlated to higher θ) is associated with a marked C_T minimum (surprisingly almost as low as in 1987), as well as low A_T (hence low C_{Tnat}), and low nitrate concentrations. These anomalies point to a change in AABW characteristics rather than a change in mixing with the underlying deep waters, and since they were associated with a decrease in C_{ant} concentrations, one may argue for an increased contribution of bottom waters ventilated far away from our study site (possibly from the Ross Sea due to higher S, Fig. 2). A few years later our data show a S minimum (correlated to lower θ), associated with a rapid increase in C_T and a rapid decrease in O_2 between 2013 and 2016, suggesting the contribution of a closer AABW such as the CDBW. The freshening of -0.01 in S that we observed on the Western side of the Kerguelen Plateau was also observed on the Eastern side of the Plateau by Menezes et al. (2017). In this region, Menezes et al. (2017) evaluated a change in salinity by about -0.008.decade^{-1} from 2007 to 2016 (against -0.002.decade^{-1} between 1994 and 2007), suggesting an acceleration of the AABW freshening in recent years. However, they also reported a warming by +0.06 °C.decade^{-1}, while we observed cooler temperature in 2016-2018. This suggests that we sampled a different mixture of AABWs.

5. Discussion

5.1. C_{ant} concentrations

In order to compare our C_{ant} estimates with other studies, we separated the 40-years time-series into 3 periods: the first period (1978-1987) corresponds to historical data when C_{ant} is expected to be low; the second period (1998-2004) starts when the first OISO cruise was conducted (and using CRMs for A_T, C_T measurements) and lasts when C_{ant} concentrations in AABW are maximum (Fig. 4a); the third period consists in the observations performed in late 2009 to 2018 when the observed variations are relatively large for S and small for C_{ant}. The mean C_{ant} concentrations for each period are 7, 14 and 13 µmol.kg^{-1}, respectively, which is consistent with the results from other studies (Table 3). The C_{ant} values for 1978-1987 can hardly be compared to other studies because very few observations were conducted in the 1980s in the SO Indian sector (Sabine et al. 1999) and because of potential biases for historical data despite their careful qualification in CARINA (Lo Monaco et al., 2010). In addition, the different methods used to estimate C_{ant} can lead to different results, especially in deep and bottom waters of the

https://doi.org/10.5194/os-2020-37
Preprint. Discussion started: 4 May 2020

298 SO (Vázquez-Rodríguez et al., 2009). Overall, Table 3 confirms that C_{ant} concentrations were low in the 1970s
299 and 1980s, and reached values of the order of 10 µmol.kg^{-1} in the 1990s, a signal not clearly captured in global
300 data-based estimates (Gruber, 1998; Sabine et al., 2004; Waugh et al., 2006; Khatiwala et al., 2013).
301 The observations presented in this analysis, although regional, offer a complement to recent estimates of C_{ant}
302 changes evaluated between 1994 and 2007 in the top 3000 m for the global ocean (Gruber et al., 2019a). In the
303 Enderby Basin at the horizon 2000-3000 m, the accumulation of C_{ant} from 1994 to 2007 is not uniform and ranges
304 between 0 and 8 µmol.kg^{-1} (Gruber et al., 2019a). At our station, in the CDW (2000-3000m) the C_{ant} concentrations
305 were not significant in 1978-1987 (-2 to 5 µmol.kg^{-1}) but increase to an average of 8.7±3.0 µmol.kg^{-1} in 1998-
306 2018 (Fig. 3a) probably due to mixing with AABW that contain more C_{ant}. Interestingly, this value is close but in
307 the high range of the C_{ant} accumulation estimated from 1994 to 2007 in deep waters of the south Indian Ocean
308 (Gruber et al., 2019a).
309 Not surprisingly, high C_{ant} concentrations are detected in the AABW formation regions (Table 3). The highest C_{ant}
310 concentrations in bottom waters (up to 30 µmol.kg^{-1}) were observed in the ventilated shelf waters in the Ross Sea
311 (Sandrini et al., 2007). In the Adélie and Mertz Polynya regions, Shadwick et al. (2014) observed high C_{ant}
312 concentrations in the subsurface shelf waters (40-44 µmol.kg^{-1}) but lower values in ALBW (15 µmol.kg^{-1}) when
313 it mixed with older CDW. In WSBW, all C_{ant} concentrations estimated from observations between 1996 and 2005
314 and with the TrOCA method (Table 3) lead to about the same values ranging between 13 and 16 µmol.kg^{-1} (Lo
315 Monaco et al., 2005b; van Heuven et al., 2011). In bottom waters formed near the Cape Darnley (CDBW), Roden
316 et al. (2016) estimated high C_{ant} concentrations in bottom waters (25 µmol.kg^{-1}) resulting from the shelf waters
317 that contain very high C_{ant} (50 µmol.kg^{-1}). The comparison with other studies confirms that far from the AABW
318 formation sites, contemporary C_{ant} concentrations are not exceeding 16 µmol.kg^{-1} on average. However, higher
319 C_{ant} concentrations are not unrealistic (Sandrini et al., 2007; Roden et al., 2016; this study in 2004) and likely
320 related to ventilation and water masses variability.
321 Table 3.

322 **5.2. C_{ant} trends and variability**

323 Comparison of long-term C_{ant} trends in deep and bottom waters of the SO is limited to very few regions where
324 repeated observations are available. To our knowledge, only 3 other studies evaluated the long-term C_{ant} trends in
325 the Southern Ocean based on more than 5 reoccupations: in the South-western Atlantic (Rios et al., 2012) and in
326 the Weddell Gyre along the Prime meridian section (van Heuven et al., 2011, 2014). Temporal changes of C_T and
327 C_{ant} have also been investigated in other SO regions, but limited to 2 to 4 reoccupations (Murata et al., 2019;
328 Williams et al., 2015; Pardo et al., 2017). Given the C_{ant} variability depicted at our location (Fig. 4a), different
329 trends can be deduced from limited reoccupations. As an example, Murata et al., (2019) evaluated the change in
330 C_{ant} from data collected 17 years apart (1994–1996 and 2012–2013) along a transect around 62°S and found a
331 small increase at our location (< 5 µmol.kg^{-1} around 60°E). This result appears very sensitive to the time of the
332 observation given that we found a minimum in C_{ant} concentrations between 2011 and 2014 (Fig. 4a) associated
333 with a marked C_T minimum (Fig. 4b). In addition, our results show that the detection of C_{ant} trends appears very
334 sensitive to the time period considered (Table 2). As an extreme case, the C_{ant} trend estimated for the period 1987-
335 2004 is +6.5 µmol.kg^{-1}.decade^{-1} (close to the theoretical C_{ant} trend of +8 µmol.kg^{-1}.decade^{-1}), but it reverses to -
336 3.5 µmol.kg^{-1}.decade^{-1} for the period 2004-2018.

https://doi.org/10.5194/os-2020-37
Preprint. Discussion started: 4 May 2020

337 The long-term C_T trend that we estimated in AABW in the eastern Enderby Basin (2.0±0.5 µmol.kg^{-1}.decade^{-1}) is
338 slightly faster than the C_T trends estimated in the WSBW in the Weddell Gyre: +1.2±0.5 µmol.kg^{-1}.decade^{-1} over
339 the period 1973-2011 and +1.6±1.4 µmol.kg^{-1}.decade^{-1} when restricted to 1996-2011 (van Heuven et al., 2014).
340 Along the SR03 line (south of Tasmania) reoccupied in 1995, 2001, 2008 and 2011, Pardo et al (2017) evaluated
341 a C_T trend of +2.4±0.2 µmol.kg^{-1}.decade^{-1} in the AABW composed of ALBW and RSBW in this sector. This is
342 higher than the C_T trends found at our location and in the Weddell Gyre, but surprisingly, this was not associated
343 with a significant increase in C_{ant}. The C_T trend in AABW along the SR03 section was likely due to the intrusion
344 of old and C_T-rich waters also revealed by an increase in silicate concentrations during 1995-2011 (Pardo et al.,
345 2017). This is a clear example of decoupling between C_T and C_{ant} trends in deep and bottom waters as observed at
346 our location in the last decade (Table 2). For C_{ant}, our 40-years trend estimate (1.6±0.6 µmol.kg^{-1}.decade^{-1}) appears
347 close to the trend reported by Rios et al. (2012) in the South-Western Atlantic AABW from 6 reoccupations
348 between 1972 and 2003 (+1.5 µmol.kg^{-1}.decade^{-1}). However, if we limit our result to the period 1978-2002 or
349 1978-2004 (about the same period as in Rios et al., 2012), our trend is much larger (+3-4 µmol.kg^{-1}.decade^{-1}).
350 At our location, the C_{ant} trend over 40 years (+1.6±0.6 µmol.kg^{-1}.decade^{-1}) explains most of the observed C_T
351 increase (+2.0±0.5 µmol.kg^{-1}.decade^{-1}). The residual of +0.4 µmol.kg^{-1}.decade^{-1} reflects changes in natural
352 processes affecting the carbon content (different AABW sources, ventilation, mixing with deep waters,
353 remineralization or carbonates dissolution). Although this is a weak signal, the natural C_T change (C_{Tnat}) mirrors
354 the observed decrease in O_2 by -0.80±0.4 µmol.kg^{-1}.decade^{-1}. This O_2 decrease detected in the Enderby Basin
355 appears to be a real feature that was documented at large scale for 1960-2010 in deep SO basins (Schmidtko et al.
356 2017), suggesting that the changes observed at 56.5°S-63°E are related to large-scale processes, possibly due to a
357 decrease in AABW formation (Purkey and Johnson, 2012).

358 **5.3. Recent C_{ant} stability**

359 Although most studies suggest a gradual accumulation of C_{ant} in the AABW, our time-series highlights significant
360 pluriannual changes, in particular over the last decade when C_{ant} concentrations were as low as around the year
361 2000 (Fig. 4a) and decoupled from the increase in C_T (Fig. 4b). This result is difficult to interpret because at our
362 location, away from AABW sources (Fig. 1), the temporal variability observed in the AABW layer can result from
363 many remote processes occurring at the AABW formation sites (such as wind forcing, ventilation, sea-ice melting,
364 thermodynamic, biological activity and air-sea exchanges), but internal processes during the transport of AABWs
365 (such as organic matter remineralization, carbonate dissolution and mixing with surrounding waters) must also be
366 taken into account. The apparent steady C_{ant} feature suggests that AABWs found at our location has stored less
367 C_{ant} in recent years. This might be linked to reduced CO_2 uptake in the AABW formation regions, as recognized
368 at large-scale in the SO from the late 1980s to 2001 (Le Quéré et al., 2007; Metzl, 2009; Lenton et al., 2012;
369 Landschützer et al., 2015). This large-scale response in the SO during a positive trend in the Southern Annular
370 Mode (SAM) is mainly associated to stronger winds driven by accelerating greenhouse gas emissions and
371 stratospheric ozone depletion, leading to warming and freshening in the SO (Swart et al., 2018), change in the
372 ventilation of the carbon-rich deep waters and reduced CO_2 uptake (Lenton et al., 2009). The reconstructed pCO_2
373 fields by Landschützer et al. (2015) suggest that the reduced CO_2 sink in the 1990s is identified at high latitudes
374 in the SO (see Fig. 2a and S9 in Landschützer et al., 2015). However, as opposed to the circumpolar open ocean
375 zone (e.g. Metzl, 2009; Takahashi et al., 2009, 2012; Munro et al., 2015; Fay et al., 2018), the long-term trend of

https://doi.org/10.5194/os-2020-37
Preprint. Discussion started: 4 May 2020

surface fCO_2 and carbon uptake deduced from direct observations are not clearly identified in the seasonal ice zone (SIZ) and shelves around Antarctica, and thus in the AABW formation regions of interest to interpret our results (Laruelle et al., 2018). There, surface fCO_2 data are sparse, especially before 1990, and cruises were mainly conducted in austral summer when the spatio-temporal fCO_2 variability is very large and driven by multiple processes at regional or small scales, such as primary production, sea-ice formation and retreat, circulation and mixing. This leads to various estimates of the air-sea CO_2 fluxes around Antarctica depending on the region and period and large uncertainty when attempting to detect long-term trends (Gregor et al., 2018).

In particular, in polynyas and AABW formation regions where fCO_2 is low and where katabatic winds prevail, very strong instantaneous CO_2 sink can occur at the local scale (up to -250 mmol $C.m^{-2}.d^{-1}$ in Terra Nova Bay in the Ross Sea according to DeJong and Dunbar, 2017). In the Prydz Bay region where CDBW is formed, recent studies show that surface fCO_2 in austral summer vary in a very large range (150-450 µatm), with the lowest fCO_2 observed in the shelf region generating very strong local CO_2 sink (-221 mmol $C.m^{-2}.d^{-1}$ according to Roden et al. 2016). The carbon uptake was particularly enhanced near Cape Darnley and coincided with the highest C_{ant} concentrations that Roden et al. (2016) estimated in the dense shelf waters that subduct to form AABW. In the Prydz Bay coastal region, surface fCO_2 values in 1993-1995 were as low as 100 µatm (Gibson and Trull, 1999) leading to a strong local CO_2 uptake of -30 mmol $C.m^{-2}.d^{-1}$ in summer. In addition, Roden et al. (2013) found a large C_T increase over 16 years (+34 $\mu mol.kg^{-1}$) in the Prydz Bay, which is much higher than the anthropogenic signal alone (+12 $\mu mol.kg^{-1}$) and likely explained by changes in primary production that would have been stronger in 1994. To our knowledge, this is the only direct observation of decadal C_T change in surface waters in a region of AABW formation (here the Prydz Bay) and it highlights the difficulty not only to evaluate the C_T and C_{ant} long-term trends in these regions but also to separate natural and anthropogenic signals when this water reaches the deep ocean. We attempted to detect long-term changes in CO_2 uptake in this region using the qualified fCO_2 data available in the SOCAT database (Bakker et al., 2016), but our estimates (not shown) were highly uncertain due to very large spatial and temporal variability. To conclude, all previous studies conducted near or in AABW formation sites clearly reveal that these regions are potentially strong carbon sinks, but how the sink changed over the last decades is not yet evaluated, and thus we are not able to certify that the recent C_{ant} stability that we observed in the AABW at our location is directly linked to the weakening of the carbon sink that was recognized at large-scale in the SO from the 1980s to mid-2000s (Le Quéré et al., 2007; Landschützer et al., 2015).

Changes in the accumulation of C_{ant} in AABW could also be directly related to changes in physical processes occurring in AABW formation region. Decadal decreasing of sea-ice production and melting of sea-ice have been documented in several regions including Cape Darnley polynyas (Tamura et al., 2016; Williams et al., 2016). The consequent changes in Antarctic surface waters properties are transmitted into the deep ocean, notably the well-recognized freshening of AABWs over the last decades (Rintoul, 2007). The warming of bottom waters was also documented in the Enderby basin (Couldrey et al., 2013) as well as at a larger scale in all deep SO basins (Purkey and Johnson, 2010; Desbruyères et al., 2016). Associated to a decrease in AABW formation in the 1990s (Purkey and Johnson, 2012), these physical changes could explain the recent stability of C_{ant} concentrations in AABW observed at our location. As AABWs from different sources spread and mix with C_T-rich deep waters before reaching our location (Fig. 1), less AABW formation and export would result in an increase in C_T (increase in C_{Tnat}) not associated with an increase in C_{ant}, and a decrease in O_2 (as observed in recent years in Fig. 4a,b,c). Finally, it is also possible that the AABW observed in recent years at our location is the result of a larger

https://doi.org/10.5194/os-2020-37
Preprint. Discussion started: 4 May 2020

contribution of older RSBW and/or ALBW that have lower C_{ant} and O_2 concentrations compared to CDBW formed at Cape Darnley and Prydz Bay.

6. Conclusion

The distribution and evolution of C_{ant} in the bottom layer of the SO are related to complex interactions between climatic forcing, air-sea CO_2 exchange at formation sites, as well as biological and physical processes during AABWs circulation. The dataset that we collected regularly in the Enderby basin over the last 20 years (1998-2018) in the frame of the OISO project, together with historical observations obtained in 1978, 1985 and 1987 (GEOSECS and INDIGO cruises), allows the investigation of C_{ant} changes in AABW over 40 years in this region. Our results suggest that the accumulation of C_{ant} explains most of (but not all) the observed increase in C_T. We also detected a decrease in O_2 that is consistent with the large-scale signal reported by Schmidtko et al. (2017), possibly due to a decrease in AABW formation (Purkey and Johnson, 2012). Our data further indicate rapid anomalies in some periods suggesting that for decadal to long-term estimates care have to be taken when analyzing the change in C_{ant} from data sets collected 10 or 20 years apart (e.g. Williams et al., 2015; Murata et al., 2019). Our results also show different C_{ant} trends on short periods, with a maximum increase of 6.5 $\mu mol.kg^{-1}.decade^{-1}$ between 1987 and 2004 and an apparent stability in the last 20 years (despite an increase in C_T). This suggests that AABWs have stored less C_{ant} in the last decade, but our understanding of the processes that explain this signal is not clear. This might be the result of the reduced CO_2 uptake in the SO in the 1990s (Le Quéré et al., 2007; Landschützer et al., 2015), but this is not yet verified from direct C_T or fCO_2 observations in AABW formation regions due to the lack of winter data and very large variability during summer. This calls for more data collection and investigations in these regions. The apparent stability of C_{ant} in AABW since 1998 could also be directly linked to a decrease in AABW formation in the 1990s (Purkey and Johnson, 2012) or a change in the contributions of AABWs from different sources, especially in the Prydz Bay region (Williams et al., 2016). In these scenarios, an increased contribution of C_T-rich and O_2-poor older CDW would also explain the decoupling between C_{ant} and C_T (increase in C_{Tnat}) and decrease in O_2 concentrations observed in recent years. The decoupling between C_{ant} and C_T is not a unique feature, as it was also reported along the SR03 section between Tasmania and Antarctica, most probably due to advection of C_T-rich waters (Pardo et al., 2017). This highlights the importance of the ocean circulation in influencing the temporal C_T and C_{ant} inventories changes (De Vries et al. 2017) and the need to better separate anthropogenic and natural variability based on time-series observations.

The evaluation and understanding of decadal C_{ant} changes in deep and bottom ocean waters are still challenging, as the C_{ant} concentrations remain low compared to C_T measurements accuracy (at best ± 2 $\mu mol.kg^{-1}$, Bockmon and Dickson, 2015) and uncertainties of data-based methods (± 6 $\mu mol.kg^{-1}$). Long-term repeated and qualified observations (at least 30 years) are needed to accurately detect and separate the anthropogenic signal from the internal ocean variability; we thus only start to document these trends that should now help to identify shortcomings in models regarding the carbon storage in the deep SO (e.g., Frölicher et al., 2014). As changes in the SO (including warming, freshening, oxygenation/deoxygenation, CO_2 and acidification) are expected to accelerate in the future in response to anthropogenic forcing and climate change (e.g. Hauck et al., 2015; Heuzé et al., 2014; Ito et al., 2015, Yamamoto et al., 2015), it is important to maintain time-series observations to complement the GO-SHIP strategy, and to occupy more regularly other sectors of the SO (Rintoul et al., 2012). In

https://doi.org/10.5194/os-2020-37
Preprint. Discussion started: 4 May 2020

this context, we hope to maintain our observations in the Southern Indian Ocean in the next decade, and with ongoing synthetic products activities such as GLODAPv2 (Olsen et al., 2016; 2019), SOCAT (Bakker et al., 2016) and more recently the SOCCOM project (Williams et al., 2018), to offer a solid database to validate ocean biogeochemical models and coupled climate/carbon models (Russell et al. 2018), and ultimately reduce uncertainties in future climate projections.

Data availability

GEOSECS, INDIGO and OISO 1998-2011 data are publicly available at the Ocean Carbon Data System (OCADS; https://www.nodc.noaa.gov/ocads/oceans/GLODAPv2_2019). OISO original data stations are available at: www.nodc.noaa.gov/ocads/oceans/RepeatSections/clivar_oiso.html. OISO 2012-2018 will be available in GLODAPv2_2021.

Author contributions

LM, CLM, NM, JF and CM performed the sampling and carried out the measurements of the OISO data. LM prepared the manuscript with contributions from CLM and NM.

Competing interests

The authors declare that they have no conflict of interest.

Acknowledgements

We thank the captains and crew of *R.S.V. Marion Dufresne* and the staff at the French Polar Institute (IPEV) for their important contribution to the success of the cruises since 1998. We are also very grateful to all colleagues, students and technicians who helped to obtain the data. We extend our gratitude to S. R. Rintoul and B. Legresy for the discussions during the preparation of the manuscript and to M. K. Shipton for the valuable comments. The OISO program is supported by the French institutes INSU and IPEV and the French program SOERE/Great-Gases. Support from the European Integrated Projects CARBOOCEAN (511176) and CARBOCHANGE (264879) is also acknowledged.

References

Álvarez, M., Lo Monaco, C., Tanhua, T., Yool, A., Oschlies, A., Bullister, J. L., Goyet, C., Metzl, N., Touratier, F., McDonagh, E. and Bryden, H. L.: Estimating the storage of anthropogenic carbon in the subtropical Indian Ocean: a comparison of five different approaches, Biogeosciences, 6(4), 681–703, doi:10/cjvsn6, 2009.

Aminot A. and Kérouel R.: Dosage automatique des nutriments dans les eaux marines : méthodes en flux continu. Ed. Ifremer, Méthodes d'analyse en milieu marin 188 pp., 2007.

Anderson, L. A. and Sarmiento, J. L.: Redfield ratios of remineralization determined by nutrient data analysis, Glob. Biogeochem. Cycle, 8(1), 65–80, doi:10/bwbg6b, 1994.

https://doi.org/10.5194/os-2020-37
Preprint. Discussion started: 4 May 2020

485 Anderson, L. G., Holby, O., Lindegren, R. and Ohlson, M.: The transport of anthropogenic carbon dioxide into
486 the Weddell Sea, J. Geophys. Res. Oceans, 96(C9), 16679–16687, doi:10/bs6f2j, 1991.

487 de Baar, H. J. W.: Options for enhancing the storage of carbon dioxide in the oceans: A review, Energy Convers.
488 Manag., 33(5), 635–642, doi:10/cqf9gd, 1992.

489 Bakker, D. C. E., Pfeil, B., Landa, C. S., Metzl, N., O'Brien, K. M., Olsen, A., Smith, K., Cosca, C., Harasawa,
490 S., Jones, S. D., Nakaoka, S., Nojiri, Y., Schuster, U., Steinhoff, T., Sweeney, C., Takahashi, T., Tilbrook, B.,
491 Wada, C., Wanninkhof, R., Alin, S. R., Balestrini, C. F., Barbero, L., Bates, N. R., Bianchi, A. A., Bonou, F.,
492 Boutin, J., Bozec, Y., Burger, E. F., Cai, W.-J., Castle, R. D., Chen, L., Chierici, M., Currie, K., Evans, W.,
493 Featherstone, C., Feely, R. A., Fransson, A., Goyet, C., Greenwood, N., Gregor, L., Hankin, S., Hardman-
494 Mountford, N. J., Harlay, J., Hauck, J., Hoppema, M., Humphreys, M. P., Hunt, C. W., Huss, B., Ibánhez, J. S. P.,
495 Johannessen, T., Keeling, R., Kitidis, V., Körtzinger, A., Kozyr, A., Krasakopoulou, E., Kuwata, A., Landschützer,
496 P., Lauvset, S. K., Lefèvre, N., Lo Monaco, C., Manke, A., Mathis, J. T., Merlivat, L., Millero, F. J., Monteiro, P.
497 M. S., Munro, D. R., Murata, A., Newberger, T., Omar, A. M., Ono, T., Paterson, K., Pearce, D., Pierrot, D.,
498 Robbins, L. L., Saito, S., Salisbury, J., Schlitzer, R., Schneider, B., Schweitzer, R., Sieger, R., Skjelvan, I.,
499 Sullivan, K. F., Sutherland, S. C., Sutton, A. J., Tadokoro, K., Telszewski, M., Tuma, M., Heuven, S. M. A. C.
500 van, Vandemark, D., Ward, B., Watson, A. J. and Xu, S.: A multi-decade record of high-quality fCO2 data in
501 version 3 of the Surface Ocean CO2 Atlas (SOCAT), Earth Syst. Sci. Data, 8(2), 383–413, doi:10/f3sgd6, 2016.

502 Benson, B. B. and Krause, D.: The concentration and isotopic fractionation of gases dissolved in freshwater in
503 equilibrium with the atmosphere. 1. Oxygen: Oxygen in freshwater, Limnol. Oceanogr., 25(4), 662–671,
504 doi:10/d5cgt8, 1980.

505 Bockmon, E. E. and Dickson, A. G.: An inter-laboratory comparison assessing the quality of seawater carbon
506 dioxide measurements, Mar. Chem., 171, 36–43, doi:10/f66mfw, 2015.

507 Brewer, P. G.: Direct observation of the oceanic CO2 increase, Geophys. Res. Lett., 5(12), 997–1000,
508 doi:10/d4tk22, 1978.

509 Broecker, W. S.: "NO", a conservative water-mass tracer, Earth Planet. Sci. Lett., 23(1), 100–107, doi:10/frw2mm,
510 1974.

511 Carmack, E. C. and Foster, T. D.: Circulation and distribution of oceanographic properties near the Filchner Ice
512 Shelf, Deep-Sea Res. Oceanogr. Abstr., 22(2), 77–90, doi:10/cm46nh, 1975.

513 Chen, C.-T. A.: On the distribution of anthropogenic CO2 in the Atlantic and Southern oceans, Deep Sea Res. Part
514 A Oceanogr. Res. Pap., 29(5), 563–580, doi:10/cfgbkb, 1982.

515 Chen, C.-T. A.: The oceanic anthropogenic CO2 sink, Chemosphere, 27(6), 1041–1064, doi:10/fndnpx, 1993.

516 Chen, C.-T. A. and Millero, F. J.: Gradual increase of oceanic CO2, Nature, 277, 205, doi:10/cwp6k7, 1979.

https://doi.org/10.5194/os-2020-37
Preprint. Discussion started: 4 May 2020

517 DeJong, H. B. and Dunbar, R. B.: Air-Sea CO2 Exchange in the Ross Sea, Antarctica, J. Geophys. Res. Oceans,
518 122(10), 8167–8181, doi:10/gcmcs3, 2017.

519 Desbruyères, D. G., Purkey, S. G., McDonagh, E. L., Johnson, G. C. and King, B. A.: Deep and abyssal ocean
520 warming from 35 years of repeat hydrography, Geophys. Res. Lett., 43(19), 10,356-10,365, doi:10/f89qrt, 2016.

521 DeVries, T., Holzer, M. and Primeau, F.: Recent increase in oceanic carbon uptake driven by weaker upper-ocean
522 overturning, Nature, 542(7640), 215–218, doi:10/f9pm4w, 2017.

523 Edmond, J. M.: High precision determination of titration alkalinity and total carbon dioxide content of sea water
524 by potentiometric titration, Deep Sea Res. and Oceanogr. Abs., 17(4), 737–750, doi:10/d496rw, 1970.

525 Fahrbach, E., Rohardt, G., Schröder, M. and Strass, V.: Transport and structure of the Weddell Gyre, Ann.
526 Geophys., 12(9), 840–855, doi:10/fxg7nh, 1994.

527 Fay, A. R., Lovenduski, N. S., McKinley, G. A., Munro, D. R., Sweeney, C., Gray, A. R., Landschuetzer, P.,
528 Stephens, B. B., Takahashi, T. and Williams, N.: Utilizing the Drake Passage Time-series to understand variability
529 and change in subpolar Southern Ocean pCO(2), Biogeosciences, 15(12), 3841–3855, doi:10/gdsttn, 2018.

530 Frölicher, T. L., Sarmiento, J. L., Paynter, D. J., Dunne, J. P., Krasting, J. P. and Winton, M.: Dominance of the
531 Southern Ocean in Anthropogenic Carbon and Heat Uptake in CMIP5 Models, J. Clim., 28(2), 862–886,
532 doi:10/w3d, 2014.

533 Fukamachi, Y., Wakatsuchi, M., Taira, K., Kitagawa, S., Ushio, S., Takahashi, A., Oikawa, K., Furukawa, T.,
534 Yoritaka, H., Fukuchi, M. and Yamanouchi, T.: Seasonal variability of bottom water properties off Adélie Land,
535 Antarctica, J. Geophys. Res. Oceans, 105(C3), 6531–6540, doi:10/c2fmvb, 2000.

536 Fukamachi, Y., Rintoul, S. R., Church, J. A., Aoki, S., Sokolov, S., Rosenberg, M. A. and Wakatsuchi, M.: Strong
537 export of Antarctic Bottom Water east of the Kerguelen plateau, Nature Geoscience, 3, 327, doi:10/cqqpng, 2010.

538 Gattuso, J.-P. and Hansson, L.: Ocean Acidification, Oxford University Press, Oxford, New York., 2011.

539 Gibson, J. A. E. and Trull, T. W.: Annual cycle of fCO2 under sea-ice and in open water in Prydz Bay, East
540 Antarctica, Mar. Chem., 66(3), 187–200, doi:10/fwg8ch, 1999.

541 Gordon, A. L.: Bottom Water Formation, in Encyclopedia of Ocean Sciences, pp. 334–340, Elsevier., 2001.

542 Gordon, A. L., Orsi, A. H., Muench, R., Huber, B. A., Zambianchi, E. and Visbeck, M.: Western Ross Sea
543 continental slope gravity currents, Deep Sea Res. Part II Top. Stud. Oceanogr., 56(13), 796–817, doi:10/bhvf5c,
544 2009.

545 Gordon, A. L., Huber, B., McKee, D. and Visbeck, M.: A seasonal cycle in the export of bottom water from the
546 Weddell Sea, Nature Geoscience, 3(8), 551–556, doi:10/bmwkr2, 2010.

https://doi.org/10.5194/os-2020-37
Preprint. Discussion started: 4 May 2020

547 Gordon, A. L., Huber, B. A. and Busecke, J.: Bottom water export from the western Ross Sea, 2007 through 2010,
548 Geophys. Res. Lett., 42(13), 5387–5394, doi:10/f7k7xb, 2015.

549 Goyet, C., Adams, R. and Eischeid, G.: Observations of the CO2 system properties in the tropical Atlantic Ocean,
550 Mar. Chem., 60(1), 49–61, doi:10/ckd593, 1998.

551 Gregor, L., Kok, S. and Monteiro, P. M. S.: Interannual drivers of the seasonal cycle of CO_2 in the Southern Ocean,
552 Biogeosciences, 15(8), 2361–2378, doi:10/gddvp8, 2018.

553 Gruber, N.: Anthropogenic CO2 in the Atlantic Ocean, Glob. Biogeochem. Cycle, 12(1), 165–191, doi:10/d2d4v8,
554 1998.

555 Gruber, N., Gloor, M., Mikaloff Fletcher, S. E., Doney, S. C., Dutkiewicz, S., Follows, M. J., Gerber, M., Jacobson,
556 A. R., Joos, F., Lindsay, K., Menemenlis, D., Mouchet, A., Müller, S. A., Sarmiento, J. L. and Takahashi, T.:
557 Oceanic sources, sinks, and transport of atmospheric CO2, Glob. Biogeochem. Cycle, 23(1), doi:10/cf59hc, 2009.

558 Gruber, N., Clement, D., Carter, B. R., Feely, R. A., Heuven, S. van, Hoppema, M., Ishii, M., Key, R. M., Kozyr,
559 A., Lauvset, S. K., Lo Monaco, C., Mathis, J. T., Murata, A., Olsen, A., Perez, F. F., Sabine, C. L., Tanhua, T. and
560 Wanninkhof, R.: The oceanic sink for anthropogenic CO2 from 1994 to 2007, Science, 363(6432), 1193–1199,
561 doi:10/gfw89w, 2019a.

562 Gruber, N., Landschützer, P. and Lovenduski, N. S.: The Variable Southern Ocean Carbon Sink, Annu. Rev. Mar.
563 Sci., 11(1), 159–186, doi:10/gf7sc9, 2019b.

564 Hall, T. M., Haine, T. W. N. and Waugh, D. W.: Inferring the concentration of anthropogenic carbon in the ocean
565 from tracers, Glob. Biogeochem. Cycle, 16(4), 78-1-78–15, doi:10/bd8qbz, 2002.

566 Hauck, J., Voelker, C., Wolf-Gladrow, D. A., Laufkoetter, C., Vogt, M., Aumont, O., Bopp, L., Buitenhuis, E. T.,
567 Doney, S. C., Dunne, J., Gruber, N., Hashioka, T., John, J., Le Quere, C., Lima, I. D., Nakano, H., Seferian, R.
568 and Totterdell, I.: On the Southern Ocean CO2 uptake and the role of the biological carbon pump in the 21st
569 century, Glob. Biogeochem. Cycle, 29(9), 1451–1470, doi:10/f7wkcs, 2015.

570 Heuzé, C., Heywood, K. J., Stevens, D. P. and Ridley, J. K.: Changes in Global Ocean Bottom Properties and
571 Volume Transports in CMIP5 Models under Climate Change Scenarios, J. Clim., 28(8), 2917–2944, doi:10/f68qt7,
572 2014.

573 Ito, T., Bracco, A., Deutsch, C., Frenzel, H., Long, M. and Takano, Y.: Sustained growth of the Southern Ocean
574 carbon storage in a warming climate, Geophys. Res. Lett., 42(11), 4516–4522, doi:10/f7jjrf, 2015.

575 Jabaud-Jan, A., Metzl, N., Brunet, C., Poisson, A. and Schauer, B.: Interannual variability of the carbon dioxide
576 system in the southern Indian Ocean (20°S–60°S): The impact of a warm anomaly in austral summer 1998, Glob.
577 Biogeochem. Cycle, 18(1), doi:10/fdtwhm, 2004.

https://doi.org/10.5194/os-2020-37
Preprint. Discussion started: 4 May 2020

578 Jiang, L.-Q., Carter, B. R., Feely, R. A., Lauvset, S. K. and Olsen, A.: Surface ocean pH and buffer capacity: past,
579 present and future, Mar. Chem., 9(1), 1–11, doi:10/ggqvrs, 2019.

580 Johnson, G. C.: Quantifying Antarctic Bottom Water and North Atlantic Deep Water volumes, J. Geophys. Res.
581 Oceans, 113(C5), doi:10/cx8cxn, 2008.

582 Johnson, G. C., Purkey, S. G. and Bullister, J. L.: Warming and Freshening in the Abyssal Southeastern Indian
583 Ocean, J. Clim., 21(20), 5351–5363, doi:10/fmr6dk, 2008.

584 Kerr, R., Goyet, C., da Cunha, L. C., Orselli, I. B. M., Lencina-Avila, J. M., Mendes, C. R. B., Carvalho-Borges,
585 M., Mata, M. M. and Tavano, V. M.: Carbonate system properties in the Gerlache Strait, Northern Antarctic
586 Peninsula (February 2015): II. Anthropogenic CO2 and seawater acidification, Deep Sea Res. Part II Top. Stud.
587 Oceanogr., 149, 182–192, doi:10/gf7sdh, 2018.

588 Key, R. M., Kozyr, A., Sabine, C. L., Lee, K., Wanninkhof, R., Bullister, J. L., Feely, R. A., Millero, F. J., Mordy,
589 C. and Peng, T. H.: A global ocean carbon climatology: Results from Global Data Analysis Project (GLODAP),
590 Glob. Biogeochem. Cycle, 18(4), GB4031, doi:10/dp7sk7, 2004.

591 Key, R. M., Olsen, A., Van Heuven, S., Lauvset, S. K., Velo, A., Lin, X., Schirnick, C., Kozyr, A., Tanhua, T.,
592 Hoppema, M., Jutterstrom, S., Steinfeldt, R., Jeansson, E., Ishi, M., Perez, F. F. and Suzuki, T.: Global Ocean Data
593 Analysis Project, Version 2 (GLODAPv2), ORNL/CDIAC-162, ND-P093,
594 doi:10.3334/CDIAC/OTG.NDP093_GLODAPv2, 2015.

595 Khatiwala, S., Primeau, F. and Hall, T.: Reconstruction of the history of anthropogenic CO2 concentrations in the
596 ocean, Nature, 462, 346, doi:10/fnz7f7, 2009.

597 Khatiwala, S., Tanhua, T., Mikaloff Fletcher, S., Gerber, M., Doney, S. C., Graven, H. D., Gruber, N., McKinley,
598 G. A., Murata, A., Ríos, A. F. and Sabine, C. L.: Global ocean storage of anthropogenic carbon, Biogeosciences,
599 10(4), 2169–2191, doi:10/f4x3rw, 2013.

600 Körtzinger, A., Mintrop, L. and Duinker, J. C.: On the penetration of anthropogenic CO2 into the North Atlantic
601 Ocean, J. Geophys. Res. Oceans, 103(C9), 18681–18689, doi:10/cjshtz, 1998.

602 Körtzinger, A., Rhein, M. and Mintrop, L.: Anthropogenic CO2 and CFCs in the North Atlantic Ocean - A
603 comparison of man-made tracers, Geophys. Res. Lett., 26(14), 2065–2068, doi:10/c9xdbf, 1999.

604 Körtzinger, A., Hedges, J. I. and Quay, P. D.: Redfield ratios revisited: Removing the biasing effect of
605 anthropogenic CO2, Limnol. Oceanogr., 46(4), 964–970, doi:10/dz32td, 2001.

606 Landschützer, P., Gruber, N., Haumann, F. A., Rödenbeck, C., Bakker, D. C. E., van Heuven, S., Hoppema, M.,
607 Metzl, N., Sweeney, C., Takahashi, T., Tilbrook, B. and Wanninkhof, R.: The reinvigoration of the Southern Ocean
608 carbon sink, Science, 349(6253), 1221, doi:10/f7q9th, 2015.

https://doi.org/10.5194/os-2020-37
Preprint. Discussion started: 4 May 2020

609 Laruelle, G. G., Cai, W.-J., Hu, X., Gruber, N., Mackenzie, F. T. and Regnier, P.: Continental shelves as a variable
610 but increasing global sink for atmospheric carbon dioxide, Nat. Commun., 9, 454, doi:10/gcxkgq, 2018.

611 Le Quéré, C., Rödenbeck, C., Buitenhuis, E. T., Conway, T. J., Langenfelds, R., Gomez, A., Labuschagne, C.,
612 Ramonet, M., Nakazawa, T., Metzl, N., Gillett, N. and Heimann, M.: Saturation of the Southern Ocean CO2 Sink
613 Due to Recent Climate Change, Science, 316(5832), 1735, doi:10/fctrq9, 2007.

614 Le Quéré, C., Andrew, R. M., Friedlingstein, P., Sitch, S., Hauck, J., Pongratz, J., Pickers, P. A., Korsbakken, J.
615 I., Peters, G. P., Canadell, J. G., Arneth, A., Arora, V. K., Barbero, L., Bastos, A., Bopp, L., Chevallier, F., Chini,
616 L. P., Ciais, P., Doney, S. C., Gkritzalis, T., Goll, D. S., Harris, I., Haverd, V., Hoffman, F. M., Hoppema, M.,
617 Houghton, R. A., Hurtt, G., Ilyina, T., Jain, A. K., Johannessen, T., Jones, C. D., Kato, E., Keeling, R. F.,
618 Goldewijk, K. K., Landschützer, P., Lefèvre, N., Lienert, S., Liu, Z., Lombardozzi, D., Metzl, N., Munro, D. R.,
619 Nabel, J. E. M. S., Nakaoka, S., Neill, C., Olsen, A., Ono, T., Patra, P., Peregon, A., Peters, W., Peylin, P., Pfeil,
620 B., Pierrot, D., Poulter, B., Rehder, G., Resplandy, L., Robertson, E., Rocher, M., Rödenbeck, C., Schuster, U.,
621 Schwinger, J., Séférian, R., Skjelvan, I., Steinhoff, T., Sutton, A., Tans, P. P., Tian, H., Tilbrook, B., Tubiello, F.
622 N., Laan-Luijkx, I. T. van der, Werf, G. R. van der, Viovy, N., Walker, A. P., Wiltshire, A. J., Wright, R., Zaehle,
623 S. and Zheng, B.: Global Carbon Budget 2018, Earth Syst. Sci. Data, 10(4), 2141–2194, doi:10/gfn48b, 2018.

624 Lenton, A., Metzl, N., Takahashi, T., Kuchinke, M., Matear, R. J., Roy, T., Sutherland, S. C., Sweeney, C. and
625 Tilbrook, B.: The observed evolution of oceanic pCO(2) and its drivers over the last two decades, Glob.
626 Biogeochem. Cycle, 26, GB2021, doi:10/gf7sd3, 2012.

627 Lo Monaco, C., Metzl, N., Poisson, A., Brunet, C. and Schauer, B.: Anthropogenic CO2 in the Southern Ocean:
628 Distribution and inventory at the Indian-Atlantic boundary (World Ocean Circulation Experiment line I6), J.
629 Geophys. Res. Oceans, 110(C6), doi:10/crcngf, 2005a.

630 Lo Monaco, C., Goyet, C., Metzl, N., Poisson, A. and Touratier, F.: Distribution and inventory of anthropogenic
631 CO2 in the Southern Ocean: Comparison of three data-based methods, J. Geophys. Res. Oceans, 110(C9),
632 doi:10/d554k3, 2005b.

633 Lo Monaco, C., Álvarez, M., Key, R. M., Lin, X., Tanhua, T., Tilbrook, B., Bakker, D. C., Van Heuven, S.,
634 Hoppema, M. and Metzl, N.: Assessing the internal consistency of the CARINA database in the Indian sector of
635 the Southern Ocean, Earth Syst. Sci. Data, 2(1), 51–70, doi:10/dtcv57, 2010.

636 Mantyla, A. and Reid, J.: On the Origins of Deep and Bottom Waters of the Indian-Ocean, J. Geophys. Res.
637 Oceans, 100(C2), 2417–2439, doi:10/cb6r8m, 1995.

638 Marshall, J. and Speer, K.: Closure of the meridional overturning circulation through Southern Ocean upwelling,
639 Nature Geoscience, 5(3), 171–180, doi:10/gf7sc5, 2012.

640 Matear, R. J.: Effects of numerical advection schemes and eddy parameterizations on ocean ventilation and oceanic
641 anthropogenic CO2 uptake, Ocean Modelling, 3(3), 217–248, doi:10/b4t667, 2001.

https://doi.org/10.5194/os-2020-37
Preprint. Discussion started: 4 May 2020

McKee, D. C., Yuan, X., Gordon, A. L., Huber, B. A. and Dong, Z.: Climate impact on interannual variability of Weddell Sea Bottom Water, J. Geophys. Res. Oceans, 116(C5), doi:10/cfcfb6, 2011.

McNeil, B. I., Matear, R. J., Key, R. M., Bullister, J. L. and Sarmiento, J. L.: Anthropogenic CO_2 Uptake by the Ocean Based on the Global Chlorofluorocarbon Data Set, Science, 299(5604), 235, doi:10/bpv29x, 2003.

Meijers, A. J. S., Klocker, A., Bindoff, N. L., Williams, G. D. and Marsland, S. J.: The circulation and water masses of the Antarctic shelf and continental slope between 30 and 80∘E, Deep Sea Res. Part II Top. Stud. Oceanogr., 57(9), 723–737, doi:10/c8qn5g, 2010.

Menezes, V. V., Macdonald, A. M. and Schatzman, C.: Accelerated freshening of Antarctic Bottom Water over the last decade in the Southern Indian Ocean, Sci. Adv., 3(1), e1601426, doi:10/gf7sbh, 2017.

Metzl, N.: Decadal increase of oceanic carbon dioxide in Southern Indian Ocean surface waters (1991–2007), Deep Sea Res. Part II Top. Stud. Oceanogr., 56(8), 607–619, doi:10/ff939g, 2009.

Metzl, N., Brunet, C., Jabaud-Jan, A., Poisson, A. and Schauer, B.: Summer and winter air–sea CO2 fluxes in the Southern Ocean, Deep Sea Res. Pt. I Oceanogr. Res. Pap., 53(9), 1548–1563, doi:10/c29cmm, 2006.

Munro, D. R., Lovenduski, N. S., Takahashi, T., Stephens, B. B., Newberger, T. and Sweeney, C.: Recent evidence for a strengthening CO2 sink in the Southern Ocean from carbonate system measurements in the Drake Passage (2002-2015), Geophys. Res. Lett., 42(18), 7623–7630, doi:10/gf7sd4, 2015.

Murata, A., Kumamoto, Y. and Sasaki, K.: Decadal-Scale Increase of Anthropogenic CO2 in Antarctic Bottom Water in the Indian and Western Pacific Sectors of the Southern Ocean, Geophys. Res. Lett., 46(2), 833–841, doi:10/gfkpzq, 2019.

Ohshima, K. I., Fukamachi, Y., Williams, G. D., Nihashi, S., Roquet, F., Kitade, Y., Tamura, T., Hirano, D., Herraiz-Borreguero, L., Field, I., Hindell, M., Aoki, S. and Wakatsuchi, M.: Antarctic Bottom Water production by intense sea-ice formation in the Cape Darnley polynya, Nature Geoscience, 6(3), 235–240, doi:10/f22qfg, 2013.

Olsen, A., Key, R. M., van Heuven, S., Lauvset, S. K., Velo, A., Lin, X., Schirnick, C., Kozyr, A., Tanhua, T., Hoppema, M., Jutterström, S., Steinfeldt, R., Jeansson, E., Ishii, M., Pérez, F. F. and Suzuki, T.: The Global Ocean Data Analysis Project version 2 (GLODAPv2) – an internally consistent data product for the world ocean, Earth Syst. Sci. Data, 8(2), 297–323, doi:10/f8377c, 2016.

Olsen, A., Lange, N., Key, R. M., Tanhua, T., Álvarez, M., Becker, S., Bittig, H. C., Carter, B. R., Cotrim da Cunha, L., Feely, R. A., Heuven, S. van, Hoppema, M., Ishii, M., Jeansson, E., Jones, S. D., Jutterström, S., Karlsen, M. K., Kozyr, A., Lauvset, S. K., Lo Monaco, C., Murata, A., Pérez, F. F., Pfeil, B., Schirnick, C., Steinfeldt, R., Suzuki, T., Telszewski, M., Tilbrook, B., Velo, A. and Wanninkhof, R.: GLODAPv2.2019 – an update of GLODAPv2, Earth Syst. Sci. Data, 11(3), 1437–1461, doi:10/ggrh7d, 2019.

Orr, J. C., Maier-Reimer, E., Mikolajewicz, U., Monfray, P., Sarmiento, J. L., Toggweiler, J. R., Taylor, N. K., Palmer, J., Gruber, N., Sabine, C. L., Quéré, C. L., Key, R. M. and Boutin, J.: Estimates of anthropogenic carbon

https://doi.org/10.5194/os-2020-37
Preprint. Discussion started: 4 May 2020

675 uptake from four three-dimensional global ocean models, Glob. Biogeochem. Cycle, 15(1), 43–60, doi:10/chb7qz,
676 2001.

677 Orr, J. C., Fabry, V. J., Aumont, O., Bopp, L., Doney, S. C., Feely, R. A., Gnanadesikan, A., Gruber, N., Ishida,
678 A., Joos, F., Key, R. M., Lindsay, K., Maier-Reimer, E., Matear, R., Monfray, P., Mouchet, A., Najjar, R. G.,
679 Plattner, G.-K., Rodgers, K. B., Sabine, C. L., Sarmiento, J. L., Schlitzer, R., Slater, R. D., Totterdell, I. J., Weirig,
680 M.-F., Yamanaka, Y. and Yool, A.: Anthropogenic ocean acidification over the twenty-first century and its impact
681 on calcifying organisms, Nature, 437(7059), 681–686, doi:10/fss432, 2005.

682 Orsi, A. H., Johnson, G. C. and Bullister, J. L.: Circulation, mixing, and production of Antarctic Bottom Water,
683 Prog. Oceanogr., 43(1), 55–109, doi:10/c7n7mx, 1999.

684 Pardo, P. C., Pérez, F. F., Khatiwala, S. and Ríos, A. F.: Anthropogenic CO2 estimates in the Southern Ocean:
685 Storage partitioning in the different water masses, Prog. Oceanogr., 120, 230–242, doi:10/f5r3v3, 2014.

686 Pardo, P. C., Tilbrook, B., Langlais, C., Trull, T. W. and Rintoul, S. R.: Carbon uptake and biogeochemical change
687 in the Southern Ocean, south of Tasmania, Biogeosciences, 14(22), 5217–5237, doi:10/gcmq92, 2017.

688 Poisson, A. and Chen, C.-T. A.: Why is there little anthropogenic CO2 in the Antarttic bottom water?, Deep Sea
689 Res. Part A Oceanogr. Res. Pap., 34(7), 1255–1275, doi:10/bq8cdr, 1987.

690 Purkey, S. G. and Johnson, G. C.: Warming of Global Abyssal and Deep Southern Ocean Waters between the
691 1990s and 2000s: Contributions to Global Heat and Sea Level Rise Budgets, J. Clim., 23(23), 6336–6351,
692 doi:10/dqf7tx, 2010.

693 Purkey, S. G. and Johnson, G. C.: Global Contraction of Antarctic Bottom Water between the 1980s and 2000s, J.
694 Clim., 25(17), 5830–5844, doi:10/f39bks, 2012.

695 Ridgwell, A. and Zeebe, R. E.: The role of the global carbonate cycle in the regulation and evolution of the Earth
696 system, Earth Planet. Sci. Lett., 234(3), 299–315, doi:10/fcp4bw, 2005.

697 Rintoul, S.R., Sparrow, M., Meredith, M.P., Wadley, V., Speer, K., Hofmann, E., Summerhayes, C., Urban, E.,
698 and Bellerby, R.: The Southern Ocean Observing System: Initial Science and Implementation Strategy. Scientific
699 Committee on Antarctic Research/Scientific Committee on Oceanic Research, 74 pp., 2012.

700 Rintoul, S. R.: Rapid freshening of Antarctic Bottom Water formed in the Indian and Pacific oceans, Geophys.
701 Res. Lett., 34(6), L06606, doi:10/dqswfv, 2007.

702 Rios, A. F., Velo, A., Pardo, P. C., Hoppema, M. and Perez, F. F.: An update of anthropogenic CO2 storage rates
703 in the western South Atlantic basin and the role of Antarctic Bottom Water, J. Mar. Syst., 94, 197–203,
704 doi:10/csg8gp, 2012.

705 Robertson, R., Visbeck, M., Gordon, A. L. and Fahrbach, E.: Long-term temperature trends in the deep waters of
706 the Weddell Sea, Deep Sea Res. Part II Top. Stud. Oceanogr., 49(21), 4791–4806, doi:10/fkm6j2, 2002.

https://doi.org/10.5194/os-2020-37
Preprint. Discussion started: 4 May 2020

707 Rodehacke, C. B., Hellmer, H. H., Beckmann, A. and Roether, W.: Formation and spreading of Antarctic deep
708 and bottom waters inferred from a chlorofluorocarbon (CFC) simulation, J. Geophys. Res. Oceans, 112(C9),
709 doi:10/dmrrts, 2007.

710 Roden, N. P., Shadwick, E. H., Tilbrook, B. and Trull, T. W.: Annual cycle of carbonate chemistry and decadal
711 change in coastal Prydz Bay, East Antarctica, Mar. Chem., 155, 135–147, doi:10/f5czpc, 2013.

712 Roden, N. P., Tilbrook, B., Trull, T. W., Virtue, P. and Williams, G. D.: Carbon cycling dynamics in the seasonal
713 sea-ice zone of East Antarctica, J. Geophys. Res. Oceans, 121(12), 8749–8769, doi:10/f9pzpx, 2016.

714 Russell, J. L., Kamenkovich, I., Bitz, C., Ferrari, R., Gille, S. T., Goodman, P. J., Hallberg, R., Johnson, K.,
715 Khazmutdinova, K., Marinov, I., Mazloff, M., Riser, S., Sarmiento, J. L., Speer, K., Talley, L. D. and Wanninkhof,
716 R.: Metrics for the Evaluation of the Southern Ocean in Coupled Climate Models and Earth System Models, J.
717 Geophys. Res. Oceans, 123(5), 3120–3143, doi:10/gdjzgh, 2018.

718 Sabine, C. L., Key, R. M., Johnson, K. M., Millero, F. J., Poisson, A., Sarmiento, J. L., Wallace, D. W. R. and
719 Winn, C. D.: Anthropogenic CO2 inventory of the Indian Ocean, Glob. Biogeochem. Cycle, 13(1), 179–198,
720 doi:10/cz2xzm, 1999.

721 Sabine, C. L., Feely, R. A., Gruber, N., Key, R. M., Lee, K., Bullister, J. L., Wanninkhof, R., Wong, C. S., Wallace,
722 D. W. R., Tilbrook, B., Millero, F. J., Peng, T.-H., Kozyr, A., Ono, T. and Rios, A. F.: The Oceanic Sink for
723 Anthropogenic CO2, Science, 305(5682), 367–371, doi:10/cbg2cq, 2004.

724 Sandrini, S., Ait-Ameur, N., Rivaro, P., Massolo, S., Touratier, F., Tositti, L. and Goyet, C.: Anthropogenic carbon
725 distribution in the Ross Sea, Antarctica, Antarct. Sci, 19(3), 395–407, doi:10/b3jnjp, 2007.

726 Schlitzer, R., Ocean data view, http://odv.awi.de, 2019.

727 Schmidtko, S., Stramma, L. and Visbeck, M.: Decline in global oceanic oxygen content during the past five
728 decades, Nature, 542, 335, doi:10/f9qh2h, 2017.

729 Shadwick, E. H., Rintoul, S. R., Tilbrook, B., Williams, G. D., Young, N., Fraser, A. D., Marchant, H., Smith, J.
730 and Tamura, T.: Glacier tongue calving reduced dense water formation and enhanced carbon uptake, Geophys.
731 Res. Lett., 40(5), 904–909, doi:10/gf7sd5, 2013.

732 Shadwick, E. H., Tilbrook, B. and Williams, G. D.: Carbonate chemistry in the Mertz Polynya (East Antarctica):
733 Biological and physical modification of dense water outflows and the export of anthropogenic CO2, J. Geophys.
734 Res. Oceans, 119(1), 1–14, doi:10/f5vcvw, 2014.

735 Siegenthaler, U. and Sarmiento, J. L.: Atmospheric carbon dioxide and the ocean, Nature, 365, 119, doi:10/fq9bjr,
736 1993.

737 Smith, N. and Treguer, P.: Physical and Chemical Oceanography in the Vicinity of Prydz Bay, Antarctica, edited
738 by S. Z. ElSayed, Cambridge Univ Press, Cambridge., 1994.

https://doi.org/10.5194/os-2020-37
Preprint. Discussion started: 4 May 2020

739 Takahashi, T., Sutherland, S. C., Wanninkhof, R., Sweeney, C., Feely, R. A., Chipman, D. W., Hales, B.,
740 Friederich, G., Chavez, F., Sabine, C., Watson, A., Bakker, D. C. E., Schuster, U., Metzl, N., Yoshikawa-Inoue,
741 H., Ishii, M., Midorikawa, T., Nojiri, Y., Koertzinger, A., Steinhoff, T., Hoppema, M., Olafsson, J., Arnarson, T.
742 S., Tilbrook, B., Johannessen, T., Olsen, A., Bellerby, R., Wong, C. S., Delille, B., Bates, N. R. and de Baar, H. J.
743 W.: Climatological mean and decadal change in surface ocean pCO(2), and net sea-air CO2 flux over the global
744 oceans, Deep-Sea Res. Part II-Top. Stud. Oceanogr., 56(8–10), 554–577, doi:10/b77k3p, 2009.

745 Takahashi, T., Sweeney, C., Hales, B., Chipman, D. W., Newberger, T., Goddard, J. G., Iannuzzi, R. A. and
746 Sutherland, S. C.: The Changing Carbon Cycle in the Southern Ocean, Oceanography, 25(3), 26–37,
747 doi:10/f4bpqs, 2012.

748 Tamura, T., Ohshima, K. I., Fraser, A. D. and Williams, G. D.: Sea ice production variability in Antarctic coastal
749 polynyas, J. Geophys. Res. Oceans, 121(5), 2967–2979, doi:10/f85drd, 2016.

750 Touratier, F. and Goyet, C.: Applying the new TrOCA approach to assess the distribution of anthropogenic CO2
751 in the Atlantic Ocean, J. Mar. Syst., 46(1), 181–197, doi:10/dm85j9, 2004a.

752 Touratier, F. and Goyet, C.: Definition, properties, and Atlantic Ocean distribution of the new tracer TrOCA, J.
753 Mar. Syst., 46(1), 169–179, doi:10/br4x3b, 2004b.

754 Touratier, F., Azouzi, L. and Goyet, C.: CFC-11, Δ14C and 3H tracers as a means to assess anthropogenic CO2
755 concentrations in the ocean, Tellus B Chem. Phys. Meteorol., 59(2), 318–325, doi:10.1111/j.1600-
756 0889.2006.00247.x, 2007.

757 Tréguer, P., and P. Le Corre: Manuel d'analyse des sels nutritifs dans l'eau de mer (utilisation de l'autoanalyseur
758 II Technicon), 2nd ed., 110 pp., L.O.C.U.B.O., Brest, 1975.

759 van Heuven, S. M. A. C., Hoppema, M., Huhn, O., Slagter, H. A. and de Baar, H. J. W.: Direct observation of
760 increasing CO2 in the Weddell Gyre along the Prime Meridian during 1973–2008, Deep Sea Res. Part II Top.
761 Stud. Oceanogr., 58(25), 2613–2635, doi:10/fh9jvz, 2011.

762 van Heuven, S. M. A. C.: Determination of the rate of oceanic storage of anthropogenic CO2 from measurements
763 in the ocean interior: The South Atlantic Ocean, Doctor of Philosophy, Groningen, 2013.

764 van Heuven, S. M. A. C., Hoppema, M., Jones, E. M. and de Baar, H. J. W.: Rapid invasion of anthropogenic CO2
765 into the deep circulation of the Weddell Gyre, Phil. Trans. R. Soc. A ou Philos. Trans. R. Soc. A-Math. Phys. Eng.
766 Sci., 372(2019), 20130056, doi:10/gf7sc6, 2014.

767 Van Wijk, E. M. and Rintoul, S. R.: Freshening drives contraction of Antarctic Bottom Water in the Australian
768 Antarctic Basin, Geophys. Res. Lett., 41(5), 1657–1664, doi:10/f5x9ff, 2014.

769 Vázquez-Rodríguez, M., Touratier, F., Lo Monaco, C., Waugh, D. W., Padin, X. A., Bellerby, R. G. J., Goyet, C.,
770 Metzl, N., Ríos, A. F. and Pérez, F. F.: Anthropogenic carbon distributions in the Atlantic Ocean: data-based
771 estimates from the Arctic to the Antarctic, Biogeosciences, 6(3), 439–451, doi:10/d8scnn, 2009.

https://doi.org/10.5194/os-2020-37
Preprint. Discussion started: 4 May 2020

772 Waugh, D. W., Hall, T. M., Mcneil, B. I., Key, R. and Matear, R. J.: Anthropogenic CO2 in the oceans estimated
773 using transit time distributions, Tellus B Chem. Phys. Meteorol., 58(5), 376–389, doi:10/bdx89x, 2006.

774 Weiss, R. F.: The solubility of nitrogen, oxygen and argon in water and seawater, Deep Sea Res. and Oceanogr.
775 Abs., 17(4), 721–735, doi:10/dxzznb, 1970.

776 Williams, G. D., Bindoff, N. L., Marsland, S. J. and Rintoul, S. R.: Formation and export of dense shelf water from
777 the Adelie Depression, East Antarctica, J. Geophys. Res. Oceans, 113(C4), C04039, doi:10/cp99bm, 2008.

778 Williams, G. D., Aoki, S., Jacobs, S. S., Rintoul, S. R., Tamura, T. and Bindoff, N. L.: Antarctic Bottom Water
779 from the Adélie and George V Land coast, East Antarctica (140–149°E), J. Geophys. Res. Oceans, 115(C4),
780 doi:10/c38prf, 2010.

781 Williams, G. D., Herraiz-Borreguero, L., Roquet, F., Tamura, T., Ohshima, K. I., Fukamachi, Y., Fraser, A. D.,
782 Gao, L., Chen, H., McMahon, C. R., Harcourt, R. and Hindell, M.: The suppression of Antarctic bottom water
783 formation by melting ice shelves in Prydz Bay, Nat. Commun., 7, 12577, doi:10/f3sfx9, 2016.

784 Williams, N. L., Feely, R. A., Sabine, C. L., Dickson, A. G., Swift, J. H., Talley, L. D. and Russell, J. L.:
785 Quantifying anthropogenic carbon inventory changes in the Pacific sector of the Southern Ocean, Mar. Chem.,
786 174, 147–160, doi:10/f7mghw, 2015.

787 Williams, N. L., Juranek, L. W., Feely, R. A., Russell, J. L., Johnson, K. S. and Hales, B.: Assessment of the
788 Carbonate Chemistry Seasonal Cycles in the Southern Ocean From Persistent Observational Platforms, J.
789 Geophys. Res. Oceans, 123(7), 4833–4852, doi:10/gd5tj8, 2018.

790 Williams, W. J., Carmack, E. C. and Ingram, R. G.: Physical Oceanography of Polynyas, in Polynyas: Windows
791 to the World, vol. 74, edited by W. O. Smith and D. G. Barber, pp. 55–85, Elsevier Science Bv, Amsterdam., 2007.

792 Yabuki, T., Suga, T., Hanawa, K., Matsuoka, K., Kiwada, H. and Watanabe, T.: Possible source of the antarctic
793 bottom water in the Prydz Bay Region, J. Oceanogr., 62(5), 649, doi:10/cbsxh9, 2006.

794 Yamamoto, A., Abe-Ouchi, A., Shigemitsu, M., Oka, A., Takahashi, K., Ohgaito, R. and Yamanaka, Y.: Global
795 deep ocean oxygenation by enhanced ventilation in the Southern Ocean under long-term global warming, Glob.
796 Biogeochem. Cycle, 29(10), 1801–1815, doi:10/f7xnvd, 2015.

797

798

799

800

801

https://doi.org/10.5194/os-2020-37
Preprint. Discussion started: 4 May 2020

802 **Table 1. List of the cruises used in this study.**

Cruise	Station	Location	Year	Month
GEOSECS	430	61.0°E / 60.0°S	1978	February
INDIGO-1	14	58.9°E / 53.0°S	1985	March
INDIGO-3	75	63.2°E / 56.5°S	1987	January
OISO-01	11	63.0°E / 56.5°S	1998	February
OISO-03	11	63.0°E / 56.5°S	1998	December
OISO-05	11	63.0°E / 56.5°S	2000	August
OISO-06	11	63.0°E / 56.5°S	2001	January
OISO-08	11	63.0°E / 56.5°S	2002	January
OISO-11	11	63.0°E / 56.5°S	2004	January
OISO-18	11	63.0°E / 56.5°S	2009	December
OISO-19	11	63.0°E / 56.5°S	2011	January
OISO-21	11	63.0°E / 56.5°S	2012	February
OISO-23	11	63.0°E / 56.5°S	2014	January
OISO-26	11	63.0°E / 56.5°S	2016	October
OISO-27	11	63.0°E / 56.5°S	2017	January
OISO-28	11	63.0°E / 56.5°S	2018	January

803
804
805
806

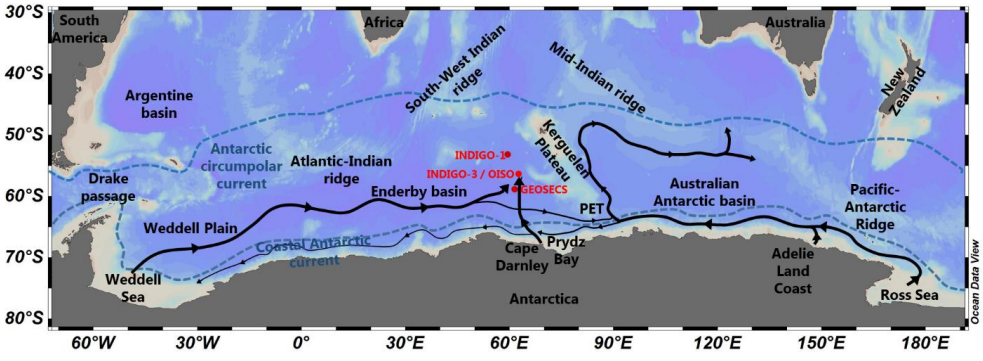

807
808 **Figure 1. The AABWs circulation from the literature (Fukamachi et al., 2010; Orsi et al., 1999) and this study, with**
809 **geographic indications (black text), SO currents (blue text and dash lines for the approximative positions) and stations**
810 **considered in this study (red text and dots). PET: Princess Elizabeth Trough. Figure produced with ODV (Schlitzer et**
811 **al., 2019).**

812

https://doi.org/10.5194/os-2020-37
Preprint. Discussion started: 4 May 2020

Ocean Science
Discussions
Open Access
EGU

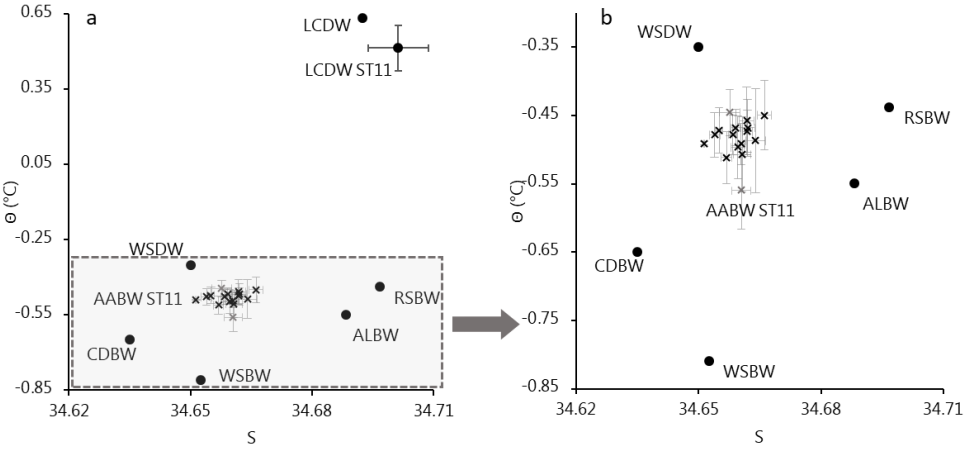

Figure 2. (a) Full Θ-S diagram of studied water masses and (b) zoomed on bottom waters. Values are from literature for the WSBW (Fukamachi et al., 2010; van Heuven, 2013; Pardo et al., 2014; Robertson et al., 2002), the WSDW (Carmack and Foster, 1975; Fahrbach et al., 1994; van Heuven, 2013; Robertson et al., 2002), the RSBW (Fukamachi et al., 2010; Gordon et al., 2015; Johnson, 2008; Pardo et al., 2014), the ALBW (Fukamachi et al., 2010; Johnson, 2008; Pardo et al., 2014), the CDBW (Ohshima et al., 2013) and the LCDW (Lo Monaco et al., 2005a; Pardo et al., 2014; Smith and Treguer, 1994), and from the OISO-ST11 dataset for the OISO-ST11 AABW and OISO-ST11 LCDW. Error bars are calculated from the individual annual averaged values for the OISO-ST11 AABW and from all data for the OISO-ST11 LCDW. For the OISO-ST11 AABW, the grey cross are the GEOSECS (lowest Θ) and INDIGO-1 (highest Θ) values.

https://doi.org/10.5194/os-2020-37
Preprint. Discussion started: 4 May 2020

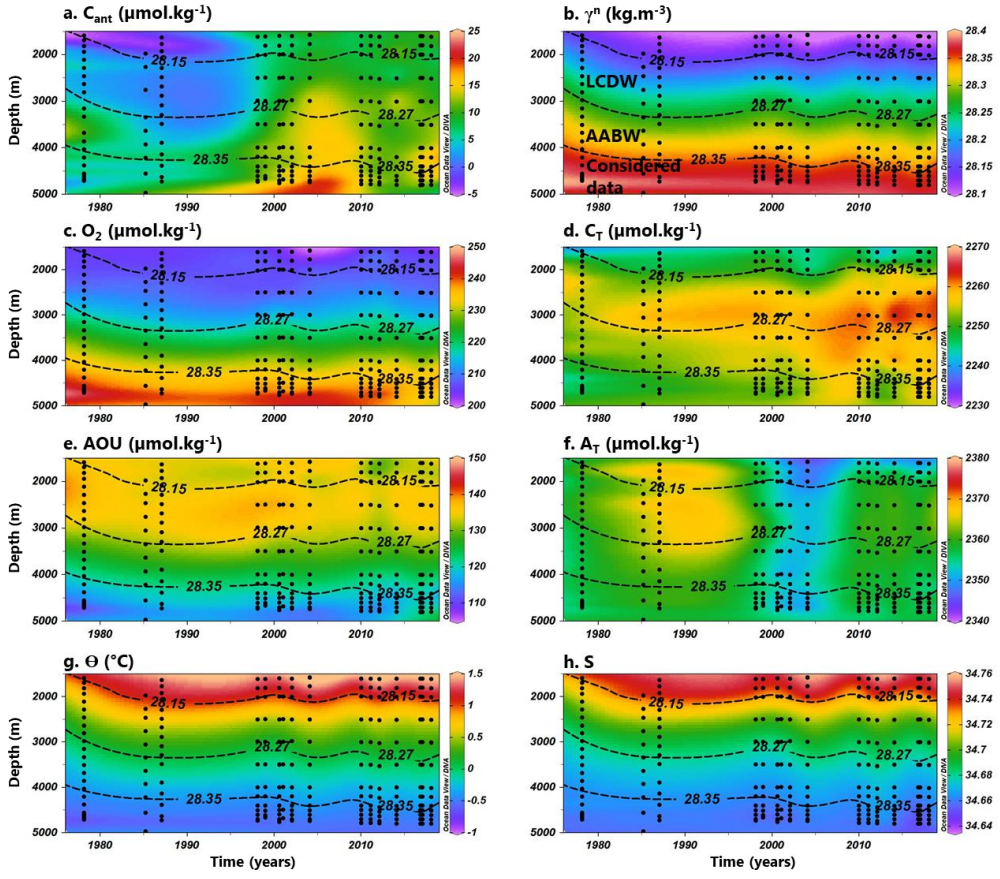

Figure 3. Hovmöller section of the carbon related properties parameters (C_{ant} via TrOCA, O_2, AOU, C_T and A_T) and hydrological properties (θ, S and γ^n) of the dataset presented in Table 1 from 1978 to 2018 and from 1500 m to the bottom. Data points are represented by the black dots. The dash isolines represent the water masses separation by γ^n detailled on the γ^n plot. Figure produced with ODV (Schlitzer et al., 2019).

https://doi.org/10.5194/os-2020-37
Preprint. Discussion started: 4 May 2020

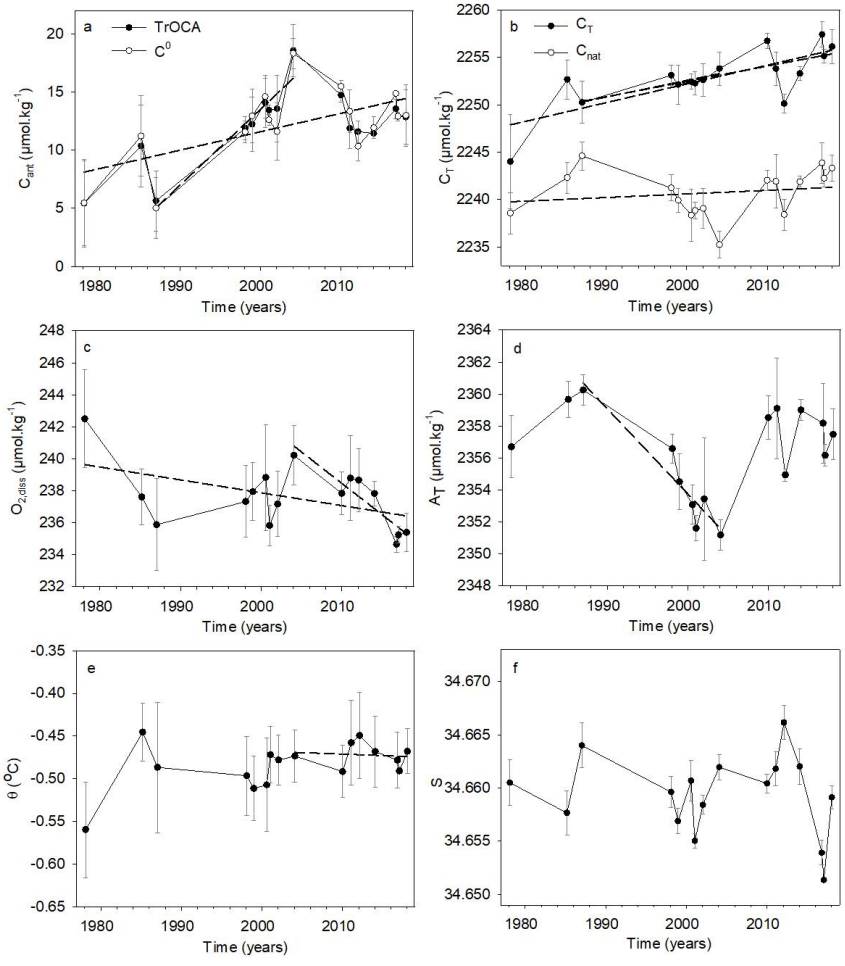

Figure 4. Interannual variability (full lines) and significant trends (at 95%, see Table 2; dotted lines) for the 40 years of observation of the OISO-ST11 AABW properties, including (a) C_{ant} by the TrOCA and the C° method, (b) C_T and C_{nat}, (c) O_2, (d) A_T, (e) Θ and (f) S.

https://doi.org/10.5194/os-2020-37
Preprint. Discussion started: 4 May 2020

Table 2: Trends (per decade) of observed and calculated properties in the AABW layer estimated over different periods (in bold: significant trends at 95% confidence level).

Period	S	Θ °C	Silicate µmol.kg^{-1}	Nitrate µmol.kg^{-1}	O_2 µmol.kg^{-1}	AOU µmol.kg^{-1}	A_T µmol.kg^{-1}	C_T µmol.kg^{-1}	C_{ant} TrOCA µmol.kg^{-1}
1978-2018	-0.001 ± 0.001	0.01 ± 0.01	-1.2 ± 0.9	0.2 ± 0.2	**-0.8 ± 0.4**	**0.7 ± 0.0**	-0.1 ± 0.1	**2.0 ± 0.5**	**1.6 ± 0.6**
1987-2018	-0.001 ± 0.001	0.01 ± 0.01	-1.9 ± 1.4	0.3 ± 0.4	-0.3 ± 0.5	0.2 ± 0.5	0.6 ± 0.1	**1.6 ± 0.5**	1.1 ± 0.8
1987-2004	-0.003 ± 0.002	0.01 ± 0.01	**-6.5 ± 1.8**	0.9 ± 0.9	1.7 ± 1.0	-1.7 ± 1.0	**-5.3 ± 0.1**	**1.8 ± 0.4**	**6.5 ± 1.0**
2004-2018	-0.006 ± 0.003	**0.02 ± 0.01**	-1.8 ± 4.5	-0.5 ± 1.0	**-3.9 ± 0.7**	**4.0 ± 0.8**	3.4 ± 0.2	1.7 ± 1.9	-3.5 ± 1.5

Table 3. Compilation of C_{ant} sequestration investigations in the AABWs ($\gamma^n \geq 28.25$ kg.m^{-3}) using the TrOCA method. The C_{ant} estimation of Pardo et al. (2014) is calculated using theoretical AABW mean composition (with 3% of ALBW) and the carbon data from the GLODAPv1 and CARINA databases. Sandrini et al. (2007) values has been measured at the bottom in the Ross Sea and correspond to recently sunk HSSW. The mean values published by Roden et al. (2016) for the AABWs present WSDW characteristics but can be a mix of CDBW and CDW.

Source	Location	Water masses considered	Year	C_{ant} µmol.kg^{-1}
Pardo et al. (2014) Fig. 5	Averaged AABW composition	WSBW-RSBW-ALBW	1994	12
Lo Monaco et al. (2005b) Fig. 4b	WOCE line I6 (30°E; 50°-70°S)	WSBW	1996	15
		CDBW		20
Sandrini et al. (2007) Fig. 4a	Ross Sea	HSSW (previous RSBW)	2002/2003	Max. of 30
Shadwick et al. (2014) Table 2	Mertz polynya and Adelie depression	ALBW	2007/2008	15
Roden et al. (2016) Table 2	South Indian ocean (30°-80°E; 60°-69°S)	WSDW-CDW-CDBW	2006	25
van Heuven et al. (2011) Fig.13	Weddell gyre (0°E; 55°-71°S)	WSBW	2005	16
This study	Enderby basin (56.5°S-63°E)	WSDW-CDBW-RSBW-ALBW	1978-1987	7 ± 3
			1987-1998	9 ± 4
			1987-2004	13 ± 4
			1998-2004	14 ± 2
			2010-2018	13 ± 1
			1978-2018	**12 ± 3**